ELSEVIER

Journal of Chemical Neuroanatomy 20 (2000) 349–374

Journal of CHEMICAL NEUROANATOMY

www.elsevier.com/locate/jchemneu

Phosphodiesterase type 4 isozymes expression in human brain examined by in situ hybridization histochemistry and [^{3}H]rolipram binding autoradiography
Comparison with monkey and rat brain

S. Pérez-Torres [a,1], X. Miró [b], J.M. Palacios [c], R. Cortés [a], P. Puigdoménech [b], G. Mengod [a,*]

[a] *Department of Neurochemistry, Instituto de Investigaciones Biomédicas de Barcelona, CSIC-IDIBAPS, c/Rosselló 161, 6a, E-08036, Barcelona, Spain*

[b] *Department Molecular Genetics, Instituto de Biologia Molecular de Barcelona, CID-CSIC, c/Jordi Girona, 18-26, E-08034, Barcelona, Spain*

[c] *Research Center, Almirall Prodesfarma SA, Cardener 68-74, E-08024, Barcelona, Spain*

Received 24 July 2000; received in revised form 20 September 2000; accepted 20 September 2000

Abstract

We have examined the distribution of four different cyclic AMP-specific phosphodiesterase isozyme (PDE4A, PDE4B, PDE4C and PDE4D) mRNAs in the brain of different species by in situ hybridization histochemistry and by autoradiography with [^{3}H]rolipram. We have compared the localization of each isozyme in human brain with that in rat and monkey brain. We have found that the four PDE4 isoforms display a differential expression pattern at both regional and cellular level in the three species. PDE4A, PDE4B and PDE4D are widely distributed in human brain, with the two latter appearing more abundant. In contrast, PDE4C in human brain, presents a more restricted distribution, limited to cortex, some thalamic nuclei and cerebellum. This is at variance with the distribution of PDE4C in rat brain, where it is found exclusively in olfactory bulb. In monkey brain, the highest expression for this isoform is found in the claustrum, and at lower levels in cortical areas and cerebellum. PDE4B presented a broad distribution, being expressed in both neuronal and non neuronal cell populations. In general, the distribution of binding sites visualized with [^{3}H]rolipram correlated well with the expression of each PDE4 isozyme.

Keywords: mRNA localization; cAMP-specific phosphodiesterase; PDE4 inhibitor; Radioligand autoradiography

1. Introduction

Intracellular cyclic adenosine 3′,5′-monophosphate (cAMP) plays an important role as a second messenger molecule controlling multiple cellular processes. It serves to transduce the action of a wide variety of neurotransmitters, hormones and can modulate signal transduction processes regulated by a range of growth factors, cytokines, and other agents. Some of the known functions of cAMP are gene transcription (Lalli and Sassone-Corsi, 1994), neurotransmitter biosynthesis (Kaufman, 1995) and release (Kandel and Schwartz, 1982), as a response regulator (Morimoto and Koshland, 1991), survival of dopaminergic neurons (Yamashita et al., 1997), synaptic facilitation and potentiation (Zhong and Wu, 1991) among others.

In order to understand the basic mechanisms underlying these functions, it is necessary to define how levels of cAMP are regulated. Its synthesis is controlled in neurons, by a variety of membrane neurotransmitter receptors, including subtypes of the dopamine, serotonin and noradrenergic receptors. These act by means of coupling of GTP-binding (G) proteins to adenylyl cyclase either to stimulate or inhibit formation of cAMP (Houslay et al., 1998). The hydrolysis of cAMP is catalyzed by a family of enzymes called phosphodi-

* Corresponding author.
E-mail address: gmlnqr@iibb.csic.es (G. Mengod).
[1] These authors have contributed equally to the work.

0891-0618/00/$ - see front matter
PII: S0891-0618(00)00097-1

esterases (PDE). Eleven members of this family have been described until present, and classified on the basis of substrate specificity, kinetic properties, sensitivity to specific inhibitors, tissue distribution and sequence derived information (Fawcett et al., 2000; Soderling and Beavo, 2000).

In this work, we have focused on the cAMP-specific phosphodiesterase 4 family (PDE4). Four kinds of PDE4 isozymes (PDE4A, PDE4B, PDE4C and PDE4D) are encoded by different gene loci, and each of them has been shown to produce several mRNAs by alternative splicing (Bolger et al., 1994). This group of isozymes is widely expressed in many tissues. These include the brain, where PDE4 is likely to be involved in processes such as control of mood, emesis and olfactory sensory transduction (Beavo, 1995). They are characterized by a low K_m, Ca^{2+}-insensitivity, specificity for cAMP as a substrate and sensitivity to the specific inhibitor rolipram.

The widespread distribution and highly tissue-specific patterns of expression of PDE4 isozymes in human tissues has opened the opportunity for the development of PDE4 inhibitors that would be useful in the treatment of human disease. Over the past decade, PDE4 inhibitor research has focused on two broad therapeutic areas, notably the CNS, with emphasis on depression, and in disorders of the immune and inflammatory systems.

Rolipram is one of the most potent and widely studied compound in the group of neuroactive cAMP-PDE inhibitors. Rolipram is a selective inhibitor of PDE4 that preferentially inhibits cAMP in brain, thus enhancing the intracellular availability of cerebral cAMP in the absence of direct stimulation of neurotransmitter receptors (Schneider, 1984; Schneider et al., 1986). Rolipram was described as a novel pharmacological approach for the treatment of endogenous depression (Watchel, 1983). Rolipram exhibits anti-depressant effects in models predictive of anti-depressant activity (Watchel and Schneider, 1986) and has been shown to be clinically effective (Zeller et al., 1984). However, its side effects (specially gastrointestinal actions, like nausea, pyrosis and emesis) due to the low degree of selectivity for the different PDE4 isoforms (Horowski and Sastre-y-Hernandez, 1985), have been the drawback for clinical application.

The aim of the present study was to map in detail the regional and cellular distribution of the four transcripts of PDE4 in human brain, in comparison with experimental animal (rodent and non-human primate). We have also studied how their distribution correlate with that of [^{3}H]rolipram binding sites (a measurement of protein expression). From the comparison between the distribution of mRNA and corresponding binding sites, inferences could be drawn on the localization of these cAMP PDEs in many brain regions.

Recent studies present evidence on the fact that specific structural differences among various members of the PDE4 family account for markedly different regulatory properties (Torphy and Page, 2000). The exquisite degree of tissue selectivity presented by PDE4 isozymes can help to obtain new classes of inhibitors by targeting to a single PDE4 isozyme.

2. Material and methods

2.1. Specimens

Adult male Wistar rats ($n = 4$) (200–300 g) were purchased from Iffa Credo (Lyon, France). The animals were killed by decapitation, brains were removed quickly, frozen on dry ice and kept at −20°C. Two male and one female monkey brains (*Macaca fascicularis*, age between 3 and 7 years old, weight range 2.4–2.7 kg, mean postmortem delay 1 h) were used. The animals were sacrificed by administration of an overdose of sodium pentobarbital. All the procedures conformed to the European Communities Council directive of November 24, 1986 (86/609/EEC). Human brain tissues (three female and one male; mean age 70-years-old, range 60–76, mean postmortem delay 10 h, range 5–23) were obtained from Neurological Tissue Bank, University of Barcelona, Hospital Clinic, (Barcelona, Spain). Human brains were from subjects without clinical or histopathological evidence of neurological or psychiatric disease. The brains were dissected, one hemisphere was sliced, frozen on dry ice and kept at −20°C. Tissue sections, 14 μm thick, were cut using a microtome-cryostat (Microm HM500 OM, Walldorf, Germany), thaw-mounted onto APTS (3-aminopropyltriethoxysilane; Sigma, St Louis, MO) coated slides, and kept at −20°C until use.

2.2. In situ hybridization histochemistry

Oligonucleotide probes for PDE4A, PDE4B, PDE4C and PDE4D were complementary to regions of each mRNA that share little similarity among the PDE family. They were purchased from Amersham Pharmacia Biotech (Little Chalfont, UK). For monkey and human, the oligonucleotides used were complementary to the following bases; 2323–2374 of the human PDE4A cDNA (GenBank acc. no. L20965); 2410–2455 of the human PDE4B cDNA (GenBank acc. no. L20971); 2333–2378 of the human PDE4C cDNA (GenBank acc. no. U66347) and 1916–1960 of the human PDE4D cDNA (GenBank acc. no. U50159). For the rat, they were complementary to bases 3649–3693 of the rat PDE4A cDNA (GenBank acc. no. L27057); 2639–2687 of the rat PDE4B cDNA (GenBank acc. no. U95748); 25–69 of the rat PDE4C

cDNA (GenBank acc. no. M25347) and 1727–1772 of the rat PDE4D cDNA (GenBank acc. no. U09455). They were 3′-end-labeled with terminal deoxynucleotidyltransferase and [^{32}P]α-dATP (3000 Ci/mmol, New England Nuclear, Boston, USA). The procedure for in situ hybridization was essentially as described earlier (Tomiyama et al., 1997). Hybridized sections were exposed to Hyperfilm β-max (Amersham) for 3–5 weeks at −70°C with intensifying screens. Duplicates of the hybridized sections were dipped in autoradiographic emulsion, Hypercoat LM-1 emulsion (Amersham). After 5–8 weeks, the emulsion was developed in Kodak D-19. Sections were examined using bright- and dark-field light microscopy (Leitz, Laborlux S, Wetzlar, Germany). For anatomical reference, the same sections or close to them were stained with cresyl violet. Brain areas and nuclei were identified using several atlases of the rat (Millhouse and Heimer, 1984; Millhouse, 1987; Paxinos, 1995; Paxinos and Watson, 1998), monkey (Szabo and Cowan, 1984; Stuart et al., 1986) and human brain (Dewulf, 1971; Nieuwenhyus et al., 1988; Paxinos, 1990; Parent, 1996).

Several routine controls were carried out to determine the specificity of the hybridization signals. For a given oligonucleotide probe, the hybridization signals were completely blocked by competition of the labeled probe with the presence of 50-fold excess of the same unlabeled oligonucleotide. Melting curve analyses showed that melting temperatures of the formed hybrids were in god agreement with the theoretically predicted values (Albretsen et al., 1988).

2.3. Acetylcholinesterase histochemistry

For anatomical reference, sections close to the ones used for in situ hybridization and radioligand binding autoradiography were stained for acetylcholinesterase activity essentially as earlier described by Karnovsky and Roots (1964).

2.4. Autoradiography

[methyl -^{3}H]rolipram (85 Ci/mmol) was purchased from Amersham. (±)-rolipram was a generous gift from Almirall Prodesfarma (Barcelona, Spain). The incubation procedure was according to that earlier published by Kaulen et al. (1989), with minor modifications. The sections were preincubated for 15 min at room temperature in 150 mM phosphate buffer, pH 7.4, containing 2 mM $MgCl_2$ and 100 μM dithiothreitol. They were then incubated for 1 h at 0°C in the same buffer with [^{3}H]rolipram 10 nM for human and 2 nM for rat. Adjacent sections were incubated in the presence of 1 μM (±)-rolipram to determine the non-specific binding. After incubation, the sections were washed twice for 5 min each in the same buffer at 0°C, dipped in distilled water at 0°C and rapidly dried under a cold air stream (4°C). Autoradiograms were generated by apposing the labeled tissue sections to a hyperfilm ^{3}H (Amersham) together with plastic ^{3}H-standards (^{3}H-Microscales, Amersham, UK) in X-ray cassettes at 4°C during 3 months for human brain sections and 4 weeks for rat brain sections.

3. Results

The specificity of labeling of [^{3}H]rolipram binding sites has been earlier documented for rat brain (Kaulen et al., 1989). [^{3}H]rolipram binding to all mammalian brain regions examined (see an example in Fig. 1A1 and C1) was completely blocked by rolipram (Fig. 1A2 and C2), in good agreement with the earlier report. Human and monkey brain sections were hybridized with the same specific oligonucleotide probes complementary to each of the PDE4 human isozyme mRNAs. Rat brain coronal sections were hybridized with the corresponding specific rat oligonucleotide probes. Fig. 1B1 shows an example of the hybridization pattern obtained with a ^{32}P-labeled oligonucleotide complementary to PDE4B mRNA in human visual cortex. Fig. 1B2 is an adjacent section, where the hybridization signals are blocked by cohybridization with an excess of the same unlabeled probe, resulting in background levels. The same is shown in Fig. 1D1 and D2 for the hybridization signal of PDE4A in the rat brain.

The four isozyme mRNAs and rolipram binding sites showed, in all species studied, a wide and differential distribution in the different brain areas examined. Table 1 summarizes the results obtained for the three species analyzed.

3.1. Distribution of PDE4 isozyme mRNAs and [^{3}H]rolipram binding sites in human brain

PDE4A, PDE4B and PDE4D transcripts presented a widespread distribution and a differential pattern throughout the human brain. In contrast, PDE4C mRNA was detected at moderate levels in a few brain areas. It is worth to notice the expression of PDE4B not only in neurons but also in white matter tracts, pia and ependymal cells.

3.1.1. Cerebral cortex

In temporal cortex PDE4A mRNA presented the highest hybridization signal (Fig. 2A2) in intermediate layers, PDE4B (Fig. 2A3) and PDE4D (in a bilaminar fashion) (Fig. 2A5) were at high levels, and PDE4C mRNA at moderate levels (Fig. 2A4). The expression in frontal and cingulate cortex was moderate for PDE4A and PDE4D, and low for PDE4B and PDE4C. In parietal cortex PDE4A, PDE4B and PDE4D were ex-

pressed at low levels whereas PDE4C was absent. Moderate levels of all four isozymes were observed in visual cortex (Fig. 2B2–B5) being PDE4B mRNA expressed at high levels in cortical white matter (Fig. 2A3 and B3). High densities of [^{3}H]rolipram binding sites were visualized through the cerebral cortex; in frontal, cingulate, parietal, temporal and visual cortex (Fig. 2A1 and B1), including white matter.

3.1.2. Basal ganglia and related areas

Weak hybridization signals for PDE4A and PDE4B mRNAs were appreciated in the head of caudate nucleus and in putamen, including the striatal cell bridge (Fig. 3A2–C2 and A3–C3). PDE4B transcripts were detected at moderate levels in magnocellular cell groups of the nucleus basalis of Meynert (Fig. 3C3), but the highest hybridization levels were seen in fiber tracts such as the capsula interna (Fig. 3A3) and anterior commissure (Fig. 3C3). The globus pallidus, presented some labeled cells for PDE4B mRNA (Fig. 3C3) with no apparent differences between the external and internal segments of the globus pallidus. Moderate hybridization signal for PDE4B mRNA could be appreciated in one of the bands of myelinated fibers in the globus pallidus; the external medullary lamina (Fig. 3C3). Low levels of PDE4D mRNA were detected in the caudate nucleus, putamen and globus pallidus. PDE4C did not show any specific hybridization signal in these nuclei. [^{3}H]rolipram binding site densities were high in putamen (Fig. 3A1–C1), striatal cell bridge (Fig. 3A1) and nucleus basalis of Meynert (Fig. 3C1), low in caudate nucleus (Fig. 3A1), globus pallidus (Fig.

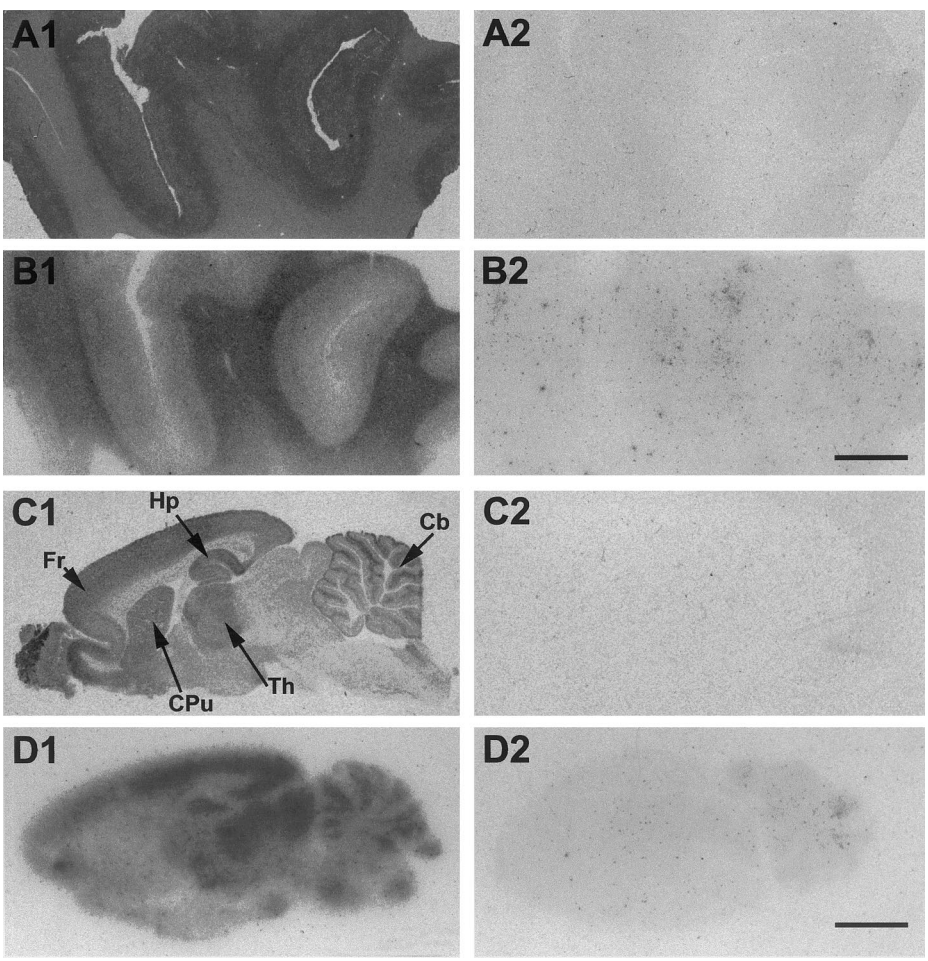

Fig. 1. Control experiments for [^{3}H]rolipram binding sites and hybridization signals in human visual cortex (A1–B2) and rat brain (C1–D2). (A1) [^{3}H]rolipram (10 nM). (A2) non-specific binding determined with 10^{-6} M (±)rolipram. (B1) Hybridization signal obtained with a ^{32}P-labeled oligonucleotide complementary to PDE4B mRNA. (B2) The hybridization signal obtained with the labeled oligonucleotide in B1 is blocked by competition with a 50-fold excess of the corresponding unlabeled probe. (C1) [^{3}H]rolipram (2 nM) binding sites in a sagittal section of the rat brain. (C2) non-specific binding determined with 10^{-6} M (±)rolipram. (D1) Hybridization signal obtained with a ^{32}P-labeled oligonucleotide complementary to PDE4A mRNA. (D2) The hybridization signal obtained with the labeled oligonucleotide in D1 is blocked by competition with a 50-fold excess of the corresponding unlabeled probe. Bar: 5 mm.

Figs. 2–5: Regional distribution of [^{3}H]rolipram binding sites and PDE4 isozyme mRNAs in several human brain regions. Pictures are digital photographs from film autoradiograms. Total binding visualized with [^{3}H]rolipram [10nM]. Distribution of PDE4A, PDE4B, PDE4C, and PDE4D mRNAs determined by in situ hybridization with the corresponding ^{32}P-labeled oligonucleotide.

Table 1
Distribution of PDE4 mRNAs and [^{3}H]rolipram binding sites in several brain regions of different species[a]

Brain Area	human brain					monkey brain				rat brain				
	PDE4A *mRNA*	PDE4B *mRNA*	PDE4C *mRNA*	PDE4D *mRNA*	[3H]Rolipram [10nM]	PDE4A *mRNA*	PDE4B *mRNA*	PDE4C *mRNA*	PDE4D *mRNA*	PDE4A *mRNA*	PDE4B *mRNA*	PDE4C *mRNA*	PDE4D *mRNA*	[3H]Rolipram [2nM]
Cerebral cortex														
Frontal cortex	++	+/++	+	++	+++	+	+	+	++	++/+++	++	-	++/+++	++
Parietal cortex	+	+	-/+	+	+++	+	+	+	++			-		
layers II,III										+/++	+++	-	++	++/+++
layer IV										+/++	++	-	+++	+
layer V										+++	++	-	+	+
layer VI										++/+++	+	-	++	+
Cingulate cortex	++	+/++	+	++	+++	+	+	+	++	++	+	-	+++	++/+++
Retrospenial cortex										+++	+	-	+++	+/++
Insular cortex						-	++	+	++					
Temporal cortex						++/+++	++/+++	+	++					
layer II,III	+/++	+/++	++/+++	+/++	++									
layer IV	+++	+++	+	+++	+++									
layer V	+/++	+/++	+	+/++	++									
layer VI	+++	+++	++	+++	+++									
Visual cortex	++	++/+++	++	++/+++	+++									
Olfactory system														
Main olfactory nucleus														
olfactory nerve										-	-	-	-	-
glomerular layer										+++	++	-	+++	+
external plexiform layer										+++	++	-	+++	+
mitral cell bodies										+++	++	-	+++	+
internal plexiform layer										+++	+	++	+++	+
internal granule cell layer										+++	+	-	+++	++/+++
Anterior olfactory nucleus										++/+++	++	-	++/+++	++
Olfactory tubercle										++	++	-	+/++	+/++
Piriform cortex										+++	+++	-	+++	+/++
Islands of Calleja										++	+/++	-	+/++	+/++
Basal ganglia and related areas														
Caudate nucleus	+/++	+	-	+	+	+	++/+++	-	+++	+	++/+++	-	+	++/+++
Putamen	++	+/++	-	+	++/+++	-	++/+++	+	++	+	++/+++	-	+	++/+++
Globus pallidus	-/+	+	-	+	+	-	++	-	++					
Claustrum	++	-	-	-	++	-	+	+++	-					
Accumbens nucleus										-/+	+++	-	-/+	+++
Nucleus basalis of Meynert	-	+/++	-	-	++/+++									
Amygdaloid complex	+	-/+	-	+	++									
medial amydaloid group										+	++/+++	-	++/++	+
amygdalopiriform area										+++	-	-	-	+
posteriomedial cortical amydaloid nucleus										++	-	-	-	-
bed nucleus of the accesory tract										-	++/+++	-	-	-
anterior cortical amygdaloid nucleus										-	++/+++	-	+/++	-
basolateral amygdaloid nucleus										-	-	-	+/++	+
Substantia nigra														
pars compacta	-/+	-	-	-/+	++/+++					++/+++	-	-	+/++	+/++
pars reticulata										++/+++	-	-	+/++	+
pars lateralis	-	-	-	-/+	++									
Paranigral nucleus	-/+	-	-	-/+	++/+++									
Septum														
Lateral septal nucleus										++	+	-	+	+++
Medial septal nucleus										++	+	-	+	-
Septohippocampal nucleus										++/+++	+	-	+	++

Table 1 (*Continued*)

Brain Area	human brain					monkey brain				rat brain				
	PDE4A *mRNA*	PDE4B *mRNA*	PDE4C *mRNA*	PDE4D *mRNA*	[3H]Rolipram [10nM]	PDE4A *mRNA*	PDE4B *mRNA*	PDE4C *mRNA*	PDE4D *mRNA*	PDE4A *mRNA*	PDE4B *mRNA*	PDE4C *mRNA*	PDE4D *mRNA*	[3H]Rolipram [2nM]
Hippocampal formation														
Taenia tecta										+++	+/++	-	+++	
Indusium griseum										+	+	-	+	+
Ammons' s horn														
stratum oriens	-	-	-	-	++/+++					-	-	-	-	+
pyramidal cell layer: CA1	+	++/++	-	++/+++	+++	+++			++	++/+++	+	-	++/+++	+++
CA2	+/++	++/+++	-	++/+++	+++	++			+++	+++	+++	-	+++	++
CA3	+++	+++	-	+++	++	++			+++	++/+++	++	-	++/+++	+
stratum radiatum	-	-	-	-	++/+++					-	-	-	-	+
stratum lacunosum-moleculare	+	+++	-	+	++/+++					+/++	+	-	++	++/+++
Dentante gyrus														
molecular cell layer	-	+	-	-	++					-	-	-	-	-
granule cell layer	+++	++	-	+++	++	++/+++			+++	++/+++	-	-	++/+++	++
polymorphic cell layer	+++	++	-	+++	+					++	+	-	++	++
Subiculum	+++	++/+++	-	++/+++	++					+++	+/++	-	++	++
Presubiculum	+++	++/+++	-	++	+/++					++/+++	+/++	-	+++	++
Parasubiculum	++	++/+++	-	++	+/++					++/+++	+/++	-	++/+++	++
Entorhinal cortex	++/+++	+++	-	++/+++	++	+++	+++	+	++	++	+/++	-	++/+++	+++
Perirhinal cortex	++/+++	+++	-	++	+/++									
Thalamus						-	++	+	-					
Reuniens thalamic nucleus										-	+++	-	-	-
Reticular thalamic nucleus	+/++	+/++	-	++/+++	++					++	+	-	+	+
Laterodorsal thalamic nucleus	-	++	+	+	+++					++/+++	+	-	++	+++
Lateroposterior thalamic nucleus	+	-	-	-	++/+++					++	-	-	+/++	+++
Central thalamic nucleus	+	-/+	-	+	-/+									
Central medial thalamic nucleus										-	+++	-	-	-
Central lateral thalamic nucleus										-	+++	-	-	-
Mediodorsal thalamic nucleus										++	-	-	+/++	++
Medial thalamic nucleus	+	+/++	+	++/+++	+++									
Medial habenular nucleus										++	++	-	+/++	++
Zona Incerta										++	+	-	++	+
Pineal gland	-	++	-	+++	++					-	+++	-	-	-
Paraventricular thalamic nucleus										-	-	-	+	-
Intermediodorsal thalamic nucleus										-	+++	-	+	-
Lateral habenular nucleus										++/+++	++	-	+++	+
Ventroposterior thalamic nucleus										++/+++	+	-	++	+++
Ventroposteriolateral thalamic nucleus	+	+	-	-/+	++	-	++	+	-					
accessory pars	+	+	-	-/+	+++									
Posterior thalamic nucleus group										+	-	-	++	+
Parafascicular thalamic nucleus	-	+	-	+	+					++	++	-	++	+
Medial pulvinar thalamic nucleus	-	+	-	++	++/+++									
Lateral pulvinar thalamic nucleus	+/++	++	-	++/+++	++/+++									
Inferior pulvinar thalamic nucleus	++	++	-	++	+									
Medial geniculate body	+/++	+	-	+/++	-					++	++	-	++/+++	++/+++
Lateral geniculate body	+++	+	-	+++	+/++	-	+/++	+	++	++	-	-	++	-
Hypothalamus														
Periventricular hypothalamic nucleus										+/++	-	-	-	-
Paraventricular hypothalamic nucleus										-	-	-	+	-
Ventromedial hypothalamic nucleus										+	+	-	+	+
Dorsomedial hypothalamic nucleus										-	+	-	-	+
Arcuate hypothalamic nucleus										+	-	-	+	+
Posterior hypothalamic nucleus										+	-	-	+	-
Mammillary complex														
suprammammilary nucleus										+++	-	-	+++	+++
medial mammillary nucleus										+++	++	-	+++	+++
lateral mammmilary nucleus										++/+++	-	-	+	-

Table 1 (*Continued*)

Brain Area	human brain					monkey brain				rat brain				
	PDE4A *mRNA*	PDE4B *mRNA*	PDE4C *mRNA*	PDE4D *mRNA*	[3H]Rolipram [10nM]	PDE4A *mRNA*	PDE4B *mRNA*	PDE4C *mRNA*	PDE4D *mRNA*	PDE4A *mRNA*	PDE4B *mRNA*	PDE4C *mRNA*	PDE4D *mRNA*	[3H]Rolipram [2nM]
Brainstem														
Superior colliculus	-	+/++	-	-	++/+++					++	+/++	-	++/+++	+
Red nucleus										-	-	-	++/+++	+
Oculomotor nucleus										++/+++	-	-	+/++	-
Supraoculomotor periaqueduct										++	-	-	++/+++	-
Interpeduncular nuclei	-	-	-	-	++/+++					+++	+	-	++/+++	+++
Pontine nuclei	+++	++	-	++	++/+++					+++	++	-	++/+++	+
Trochlear nucleus	-	-	-	-	+++									
Dorsal raphe	-	-	-	-	+++					-	-	-	++	+
Parabigeminal nucleus										++	++	-	++	++
Reticulotegmental nucleus of the pons										++/+++	-	-	++	-
Pedunculopontine tegmental nucleus										++/+++	-	-	-	-
Periolivary nuclei										++	-	-	++	-
Ventral tegmental nucleus										+++	-	-		-
Superior olive	-	+	-	-	++									
Trapezoid body										++	-	-	++	-
Raphe magnus nucleus	-	-	-	-	++					-	-	-	+	-
Prepositus hypoglossal nucleus										+	-	-	+	-
Abducens nucleus	-	-	-	-	+++									
Facial nucleus	-	-	-	-	++/+++					+	-	-	++	+
Dorsal cochlear nucleus										++	+/++	-	++/+++	+/++
Nucleus of the solitary tract	-	++/+++	-	++/+++	+++					+/++	+	-	++	+++
Vestibular nuclei														
lateral nucleus												-	+++	+
medial nucleus										++	+	-	+++	+
spinal nucleus										++	+	-	+++	+
Spinal trigeminal nucleus (Sp5)	-	+/++	-	++	+++					++/+++	++/+++	-	++/+++	+
Inferior olivary complex										-	+++	-	-	++/+++
medial nucleus (IOM)	-	+	-	+	++									
principal nucleus (IOPr)	-	++	-	+++	++/+++									
Hypoglossal nucleus	-	+	-	-	+++					+	-	-	++	-
Lateroreticular nucleus	-/+	+	-	+/++	++/+++					+/++	-	-	+/++	-
Cuneate nucleus	-	+	-	+/++	++/+++					++	+	-	++	+/++
Area postrema										-	++	-	+++	+/++
Gracile nucleus	-	+	-	+	++/+++					++	+	-	++	+/++
gelatinous layer of the caudal Sp5	-/+	+++	-	+++	+++									
Spinal accessory (supraspinal) nucleus	-	+	-	+	++									
Cerebellum														
molecular layer	-	-	-	-	+++					-	-	-	-	++/+++
granular layer	+++	+++	++/+++	+++	++/+++	+++	++	+	+++	++	+++	-	+++	++
purkinje cells	-	+++	-	+++	-					-	-	-	-	-
white matter	-	++	-	-	++	-	++	-	-	-	++	-	-	-
Cerebellar nuclei	+	+	-	+	++/+++	+	+++	-	++	+/++	-	-	++/+++	+
Non neuronal regions														
Genus corpus callosum										-	++/+++	-	-	+
Cerebral peduncle										-	++	-	-	+
Anterior commissure	-	+++	-	-	+					-	+	-	-	-
Capsula interna	-	++/+++	-	-	-									
Angular bundle	-	+++	-	-	-									
Fimbria	-	++/+++	-	-	+									

[a] The levels of intensity are indicated from '+' for low intensity up to '++' for highest intensity. '−' marks not detected, white empty boxes indicates not examined.

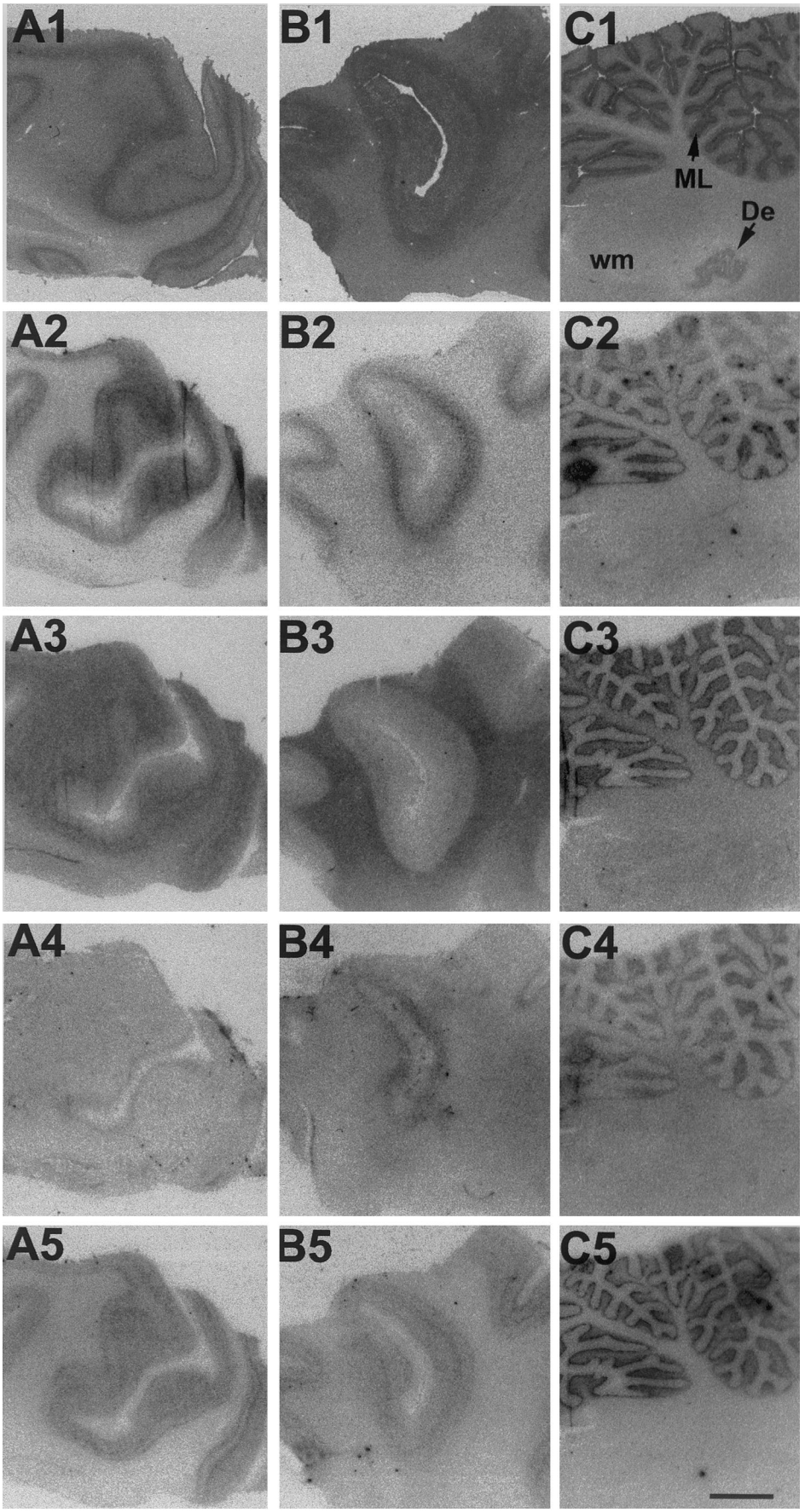

Fig. 2.

3C1), external medullary lamina (Fig. 3C1) and white matter tracts. PDE4A mRNA was the only PDE4 isozyme expressed in claustrum (Fig. 3B2) where moderate densities of [^{3}H]rolipram binding sites were also observed (Fig. 3B1).

The paranigral nucleus was clearly enriched in [^{3}H]rolipram binding sites, high densities were also visualized in densely packed neurons of the substantia nigra pars compacta, whereas, in the pars lateralis they were present at moderate levels (Fig. 3D1), where, in contrast, no hybridization signal for any PDE4 isozyme could be detected.

3.1.3. Hippocampal formation

High levels of PDE4A, PDE4B and PDE4D mRNAs were detected in the entire hippocampal formation (Fig. 4A2–A4), PDE4C did not show any specific hybridization signal.

PDE4A, PDE4B and PDE4D mRNAs were present at high levels in the pyramidal cell layer of CA2 (Fig. 4A2–A4). They were also expressed in CA3 and CA1 fields, being PDE4A at lower levels than the others. In the granule and the polymorphic cell layers of dentate gyrus strongly labeled cells were detected for PDE4A, PDE4B and PDE4D, low expression in the stratum lacunosum-moleculare, except PDE4B that presented high expression levels. Again, PDE4B mRNA was widely found in the white matter and in many fibers tracts, as fimbria and angular bundle (Fig. 4A3).

In the subicular complex, strong hybridization signals for PDE4A, PDE4B and PDE4D could be observed in the pyramidal cell layer of the subiculum (Fig. 4A2–A4) and in layer II of pre- and parasubiculum. The entorhinal cortex was clearly enriched in these three isozymes, PDE4A mRNA was present at high levels in layers III and V (Fig. 4A2), and at lower levels in layers II and VI. Moderate to high hybridization signal for PDE4B mRNA was visualized in layer V, and lower in the rest of the layers (Fig. 4A3). PDE4D mRNA showed also high levels of hybridization in layer V and cell islands of layer II (Fig. 4A4), and a few labeled cells in layer III. In addition, the perirhinal cortex showed moderate to high levels of both PDE4A and PDE4B mRNAs, whereas, PDE4D mRNA was detected at lower levels (Fig. 4A2–A4).

High densities of [^{3}H]rolipram binding sites were found in the pyramidal cells layers of CA1 and CA2, while binding density was moderate in the CA3 (Fig. 4A1). Binding sites were also seen at high densities in stratum oriens, stratum radiatum and stratum lacunosum-moleculare of CA1 and CA2 fields, at moderate densities in the molecular and granule cell layer of dentate gyrus, and lower in the polymorphic cell layer. Moderate binding site densities were also detected in subiculum, pre- and parasubiculum as well as in both entorhinal and perirhinal cortex, with no apparent gradient among the different layers. The silver grain intensity of autoradiograms was lower over the white matter, fiber tracts, and fimbria (Fig. 4A1).

Low levels of PDE4A, PDE4B and PDE4D mRNA were detectable in the amygdaloid nuclei. [^{3}H]rolipram binding sites were present at moderate densities in these nuclei (Table 1).

3.1.4. Thalamus

Low levels of PDE4A mRNA were observed in many nuclei of the anterior part of the thalamus (Fig. 4B2), such as the lateroposterior, the medial, the central and the ventral posteriolateral (including its accesory pars) thalamic nuclei. In contrast, moderate levels of PDE4A transcripts were detectable in the posterior thalamic nuclei (Fig. 4C2), lateral pulvinar and inferior nuclei. No hybridization signal was detected in the medial pulvinar nucleus.

PDE4B probe hybridized at moderate levels in the laterodorsal and medial nuclei. Low levels were found in the accesory pars of the ventral posteriolateral nucleus, the central and the parafascicular nuclei (Fig. 4B3). In the posterior thalamic nuclei (Fig. 4C3), moderate levels were observed in the lateral and inferior pulvinar nuclei, being lower in the medial pulvinar nucleus.

PDE4C transcripts were only found at low intensity in a few thalamic nuclei, like the medial and the laterodorsal thalamic nuclei (Table 1).

In the anterior thalamic nuclei (Fig. 4B4), PDE4D mRNA showed moderate hybridization levels in medial nucleus, low levels in laterodorsal, central and parafascicular nuclei. Expression of PDE4D mRNA was also seen in the posterior thalamic nuclei (Fig. 4C4), being higher in the lateral pulvinar than in both inferior and medial pulvinar.

Remarkable densities of [^{3}H]rolipram binding sites were observed throughout the thalamic nuclei. In the anterior thalamic nuclei (Fig. 4B1), high densities were observed in the accesory pars of ventral posteriolateral nucleus, as well as in the laterodorsal and medial nuclei. Moderate to high levels were also found in the lateroposterior nucleus. Lower binding site densities were detected in the central and parafascicular nuclei. Con-

Fig. 2. Regional distribution of [^{3}H]rolipram binding sites and PDE4 isozyme mRNAs in human cortex (A1–A5, temporal, and B1–B5, visual) and cerebellum (C1–C5). A1–Cl, [^{3}H]rolipram binding sites; A2–C2, PDE4A mRNA; A3–C3, PDE4B mRNA; A4-C4, PDE4C mRNA; A5–C5, PDE4D mRNA. Note the high density of binding sites in the molecular layer of the cerebellum and the strong hybridization signal for PDE4B mRNA in the white matter. Bar: 5 mm.

cerning the posterior thalamic nuclei (Fig. 4C1), moderate to high densities of binding sites were observed in the lateral and medial pulvinar nuclei, being lower in the inferior pulvinar.

The reticular nucleus presented a typical pattern of PDE4 expression (Fig. 4, panels B and C). Both PDE4A and PDE4B mRNA showed moderate levels in the posterior part of the reticular nucleus, with lower levels detected in its anterior part. Similar pattern of PDE4D transcripts and [^{3}H]rolipram binding sites were observed, but at higher levels. No hybridization signal of PDE4C mRNA was seen in this nucleus.

Both PDE4A and PDE4D mRNA were present at high levels in the six main laminae of the lateral geniculate body. High hybridization signals of both transcripts were mainly seen in the multipolar cells of the six laminae, without apparent differences between the pars magnocellular and pars parvocellular. Low levels were detected in the medial geniculate body, mainly in the dorsal and ventral divisions (Fig. 4C2 and C4, respectively). Few PDE4B mRNA labeled cells were appreciated in the medial geniculate body (mainly in dorsal and ventral division) as well as in the different laminae of the lateral geniculate body (Fig. 4C3). [^{3}H]rolipram binding sites were visualized in the different laminae of lateral geniculate body at intermediate to low densities (Fig. 4C1).

3.1.5. Brainstem

Pontine nuclei expressed PDE4A, PDE4B and PDE4D mRNAs (Fig. 5A2–A4). PDE4B presented a diffuse hybridization signal in the reticular (ventral, medial and dorsal) nuclei (Fig. 5B3). Somatosensory nuclei, such as the cuneate, the gracile and the spinal trigeminal showed intermediate hybridization signals for PDE4B (Fig. 5B3 and C3) and for PDE4D (Fig. 5B4 and C4). The hypoglossal nucleus weakly expressed PDE4B mRNA. In addition, moderate levels of PDE4B mRNA were observed in the inferior olivary complex, including the principal and medial nuclei where also high hybridization signal for PDE4D was seen, specially in the principal nucleus (Fig. 5B3 and B4, respectively). In the nucleus of the solitary tract, both PDE4B and PDE4D transcripts were detected in the different subnuclei. Moderate to high levels were visualized in both paracommissural and commissural solitary nuclei

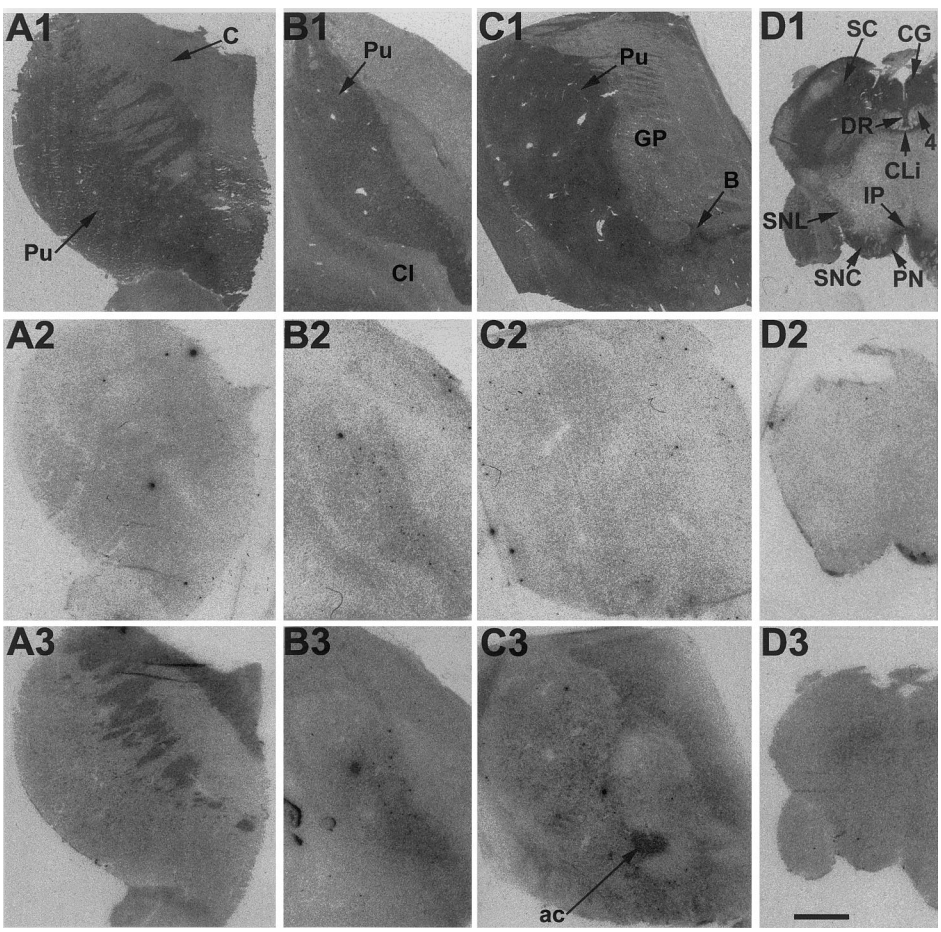

Fig. 3. Distribution of [^{3}H]rolipram binding sites (A1–D1), PDE4A mRNA (A2–D2), and PDE4B mRNA (A3–D3) in human basal ganglia. Note the presence of PDE4B mRNA in the nucleus basalis of Meynert and the anterior commissure. Bar: 5 mm.

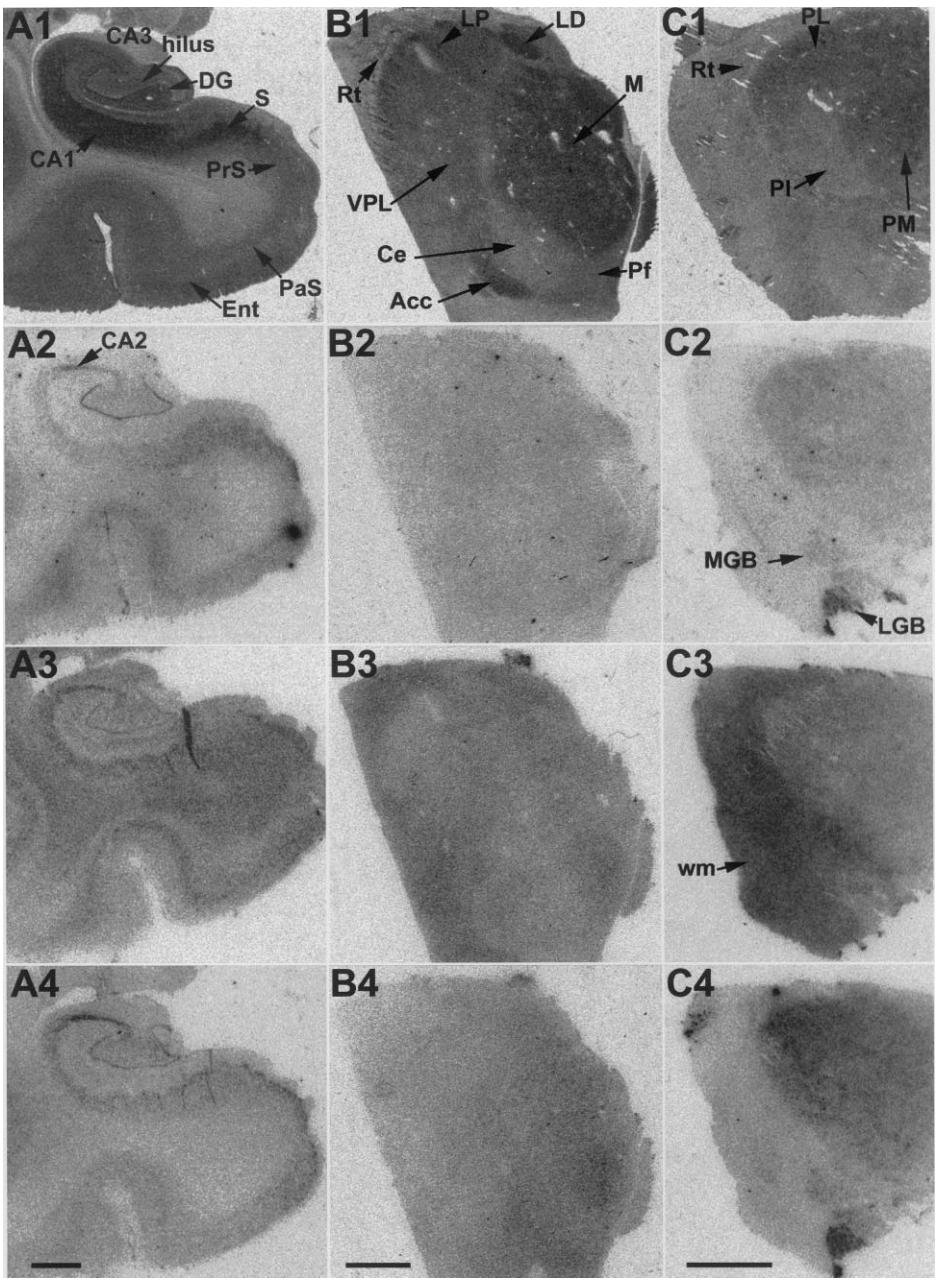

Fig. 4. Visualization of [^{3}H]rolipram binding sites and several PDE4 mRNAs in the hippocampal formation (A1–A4), the anterior thalamic nuclei (B1–B4) and the posterior thalamic nuclei (C1–C4) of the human brain. A1-C1, [^{3}H]rolipram binding sites; A2–C2, PDE4A mRNA; A3–C3, PDE4B mRNA; A4–C4, PDE4D mRNA. Note the high density of binding sites in many thalamic nuclei and the high levels of expression of PDE4D mRNA in the corpus geniculatum laterale. Bar in A4: 2 mm (A4 = A1 = A2 = A3). Bar in B4: 3 mm (B4 = B1 = B2 = B3). Bar in C4: 4 mm (C4 = C1 = C2 = C3).

and lower levels in the intermediate solitary nucleus (Fig. 5B3 and B4, respectively). No hybridization signal for PDE4A mRNA could be observed in the solitary tract (Fig. 5B2).

[^{3}H]rolipram binding sites were visualized at high concentrations in the interpeduncular (Fig. 3D1), and in the pontine nuclei, including the longitudinal fiber bundles of the pontine nucleus, mostly the corticospinal tract. Intermediate densities were found in the raphe magnus (Fig. 5A1), whereas, higher densities were observed in dorsal raphe nucleus, caudal linear nucleus of the raphe and superior colliculus (Fig. 3D1).

High densities of [^{3}H]rolipram binding sites were observed in different nuclei of the motor cranial nerves; the hypoglossal (Fig. 5B1), facial, and abducens nuclei (Fig. 5A1). High densities were found in both paracommissural and commissural solitary nuclei, whereas, moderate densities were observed in the intermediate nucleus as well as the solitary tract (Fig. 5B1). The silver grain intensity was moderate over the cuneate

nucleus, mostly in the rotunda and triangular part, as well as in the external cuneate nucleus. Intermediate densities of [^{3}H]rolipram binding sites were also visualized in the lateral reticular nuclei, gracile nucleus and in the inferior olivary complex with the principal nucleus of the olivary complex presenting higher densities of binding sites than the medial nucleus (Fig. 5B1). Low binding densities were also visualized in the superior olivary nucleus (Fig. 5A1).

The pineal gland showed high levels of PDE4D mRNA; two types of cells could be differentiated — large and strongly labeled cells arranged in lobules, and small cells with low labeling. Moderate levels of PDE4B transcript were also observed in this gland with no apparent distinction between the two types of cells. No hybridization signal of both PDE4A and PDE4C mRNA were detectable. Moderate concentrations of [^{3}H]rolipram binding sites were also visualized in the pineal gland (Table 1).

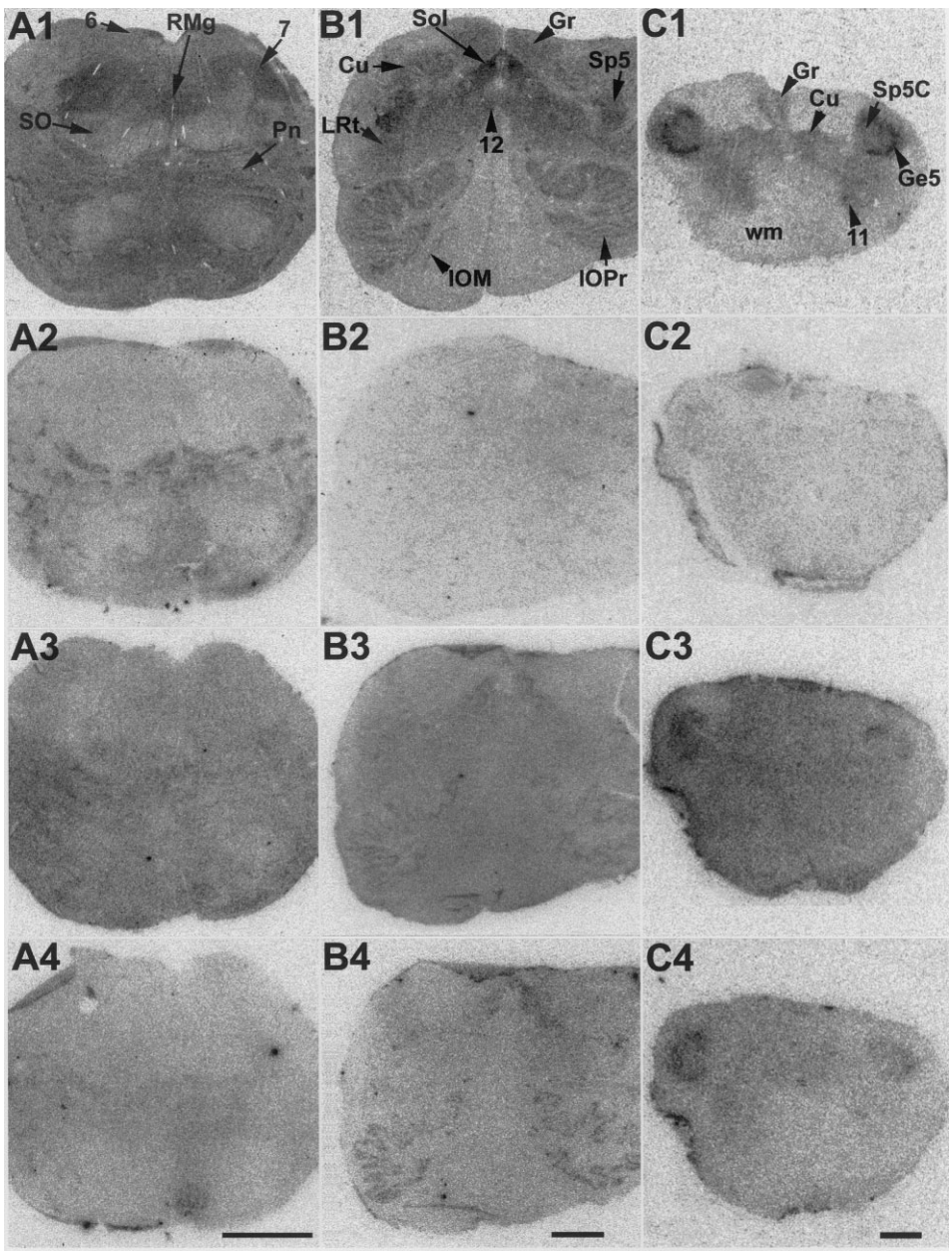

Fig. 5. Visualization of [^{3}H]rolipram binding sites and several PDE4 mRNAs at different levels of the human brainstem. A1–C1; [^{3}H]rolipram binding sites. A2–C2, PDE4A mRNA; A3–C3, PDE4B mRNA. A4–C4, PDE4D mRNA. Note the absence of PDE4A mRNA in the spinal cord and the high levels of hybridization signal for PDE4D mRNA in the inferior olive as well as in the gelatinous layer of the spinal trigeminal nucleus. Bar in A4: 3 mm (A4 = A1 = A2 = A3). Bar in B4: 3 mm (B4 = B1 = B2 = B3). Bar in C4: 2 mm (C4 = C1 = C2 = C3).

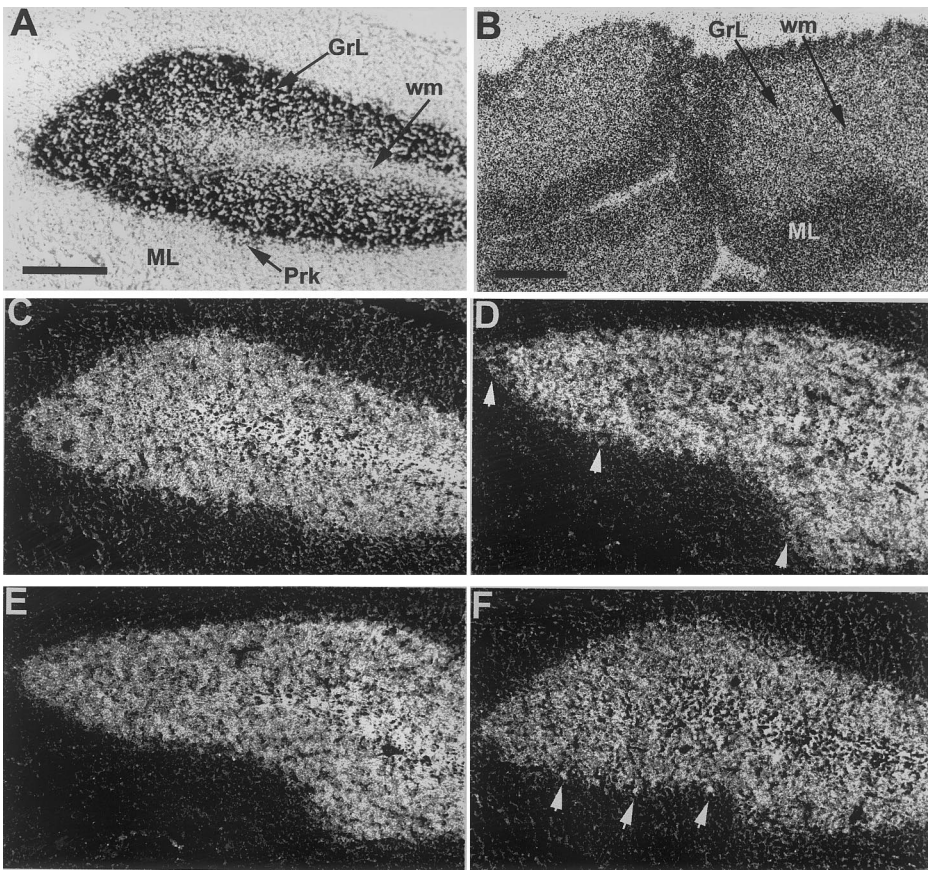

Fig. 6. Comparison of the distribution of [^{3}H]rolipram binding sites and PDE4 isozyme mRNAs in the human cerebellum. (A) is a bright-field photomicrograph of the cerebellar cortex stained with cresyl violet. (B) is a bright field photomicrograph from film autoradiogram with [^{3}H]rolipram [10 nM]. (C–F) are dark-field photomicrographs from emulsion-dipped sections showing the presence of PDE4A (C), PDE4B (D), PDE4C (E) and PDE4D (F) mRNA. Note the presence of high densities of [^{3}H]rolipram binding sites in the molecular layer and the labeling of PDE4B and PDE4D mRNA in the Purkinje cells. Bar in A: 0.3 mm (A = C = D = E = F). Bar in B: 0.5 mm.

3.1.6. Spinal cord

High hybridization signals for PDE4B (Fig. 5C3) and PDE4D mRNA (Fig. 5C4) and low for PDE4A mRNA (Fig. 5C2) were observed in the gelatinous layer of the caudal spinal trigeminal nucleus. Few labeled cells containing PDE4B and PDE4D mRNAs were detectable in the spinal accessory nucleus (Fig. 5C3 and C4). PDE4B mRNA was also seen in the white matter (Fig. 5C3). PDE4C mRNA was not detected in the spinal cord. Very high densities of [^{3}H]rolipram binding sites were visualized in the gelatinous layer of the caudal spinal trigeminal nucleus and moderate densities were seen in the spinal accessory nucleus (Fig. 5C1). The spinal trigeminal nucleus presented high densities of [^{3}H]rolipram binding sites, in particular, in the caudal pars of this nucleus (Fig. 5B1). These high densities were extending caudally as far as the second cervical spinal segment, reaching the highest levels in the substantia gelatinosa (Fig. 5C1). Low densities of binding sites were visualized in the interpolar pars of the spinal trigeminal nucleus.

3.1.7. Cerebellum

High levels of hybridization of PDE4A (Fig. 2C2 and 6C), PDE4B (Fig. 2C3 and 6D) and PDE4D (Fig. 2C5 and 6F) mRNA were seen in the granule cell layer of the cerebellum, whereas no signal was detected in the molecular layer. The only specific hybridization signal of PDE4C mRNA was detected at moderate levels in the granule cell layer of the cerebellum (Fig. 2C4 and 6E). Purkinje cells were labeled for PDE4B and PDE4D mRNA (Fig. 6D and F, respectively). High densities of [^{3}H]rolipram binding sites were visualized in the granule cell layer of the cerebellum, although the silver grain intensity of autoradiograms was much higher in the molecular layer of the cerebellum (Fig. 2C1 and 6B). In addition, both PDE4B mRNA (Fig. 2C3) and [^{3}H]rolipram binding sites were detectable at moderate levels in the white matter (Fig. 2C1). The dentate nucleus presented moderate to high concentrations of [^{3}H]rolipram binding sites (Fig. 2C1), whereas, PDE4A (Fig. 2C2), PDE4B (Fig. 2C3) and PDE4D (not shown) mRNAs were detected at low levels.

3.2. Distribution of PDE4 isozyme mRNAs in monkey brain

Monkey brain coronal sections were hybridized with the same specific oligonucleotide probes complementary to each of the PDE4 human isozyme mRNAs. PDE4A, PDE4B, and PDE4D mRNAs were detected in relatively high concentrations in many brain areas, whereas, PDE4C mRNA expression was seen in more restricted brain areas.

3.2.1. Cerebral cortex

Both PDE4A and PDE4B mRNA were detected at high levels in temporal cortex, and at low levels in frontal, cingular and parietal cortex. In addition, moderate levels of expression of PDE4B mRNA were also seen in the insular cortex (Fig. 7A2 and A3). Both PDE4C and PDE4D mRNA presented moderate levels of hybridization signal in the entire cerebral cortex (Fig. 7A4 and A5).

3.2.2. Basal ganglia and related areas

PDE4B mRNA were present at intermediate density in the putamen and also in the globus pallidus (Fig. 7A3). The claustrum was the region, where PDE4C mRNA exhibited the highest levels of expression (Fig. 7A4).

3.2.3. Hippocampal formation

Moderate levels of PDE4A mRNA were seen in the pyramidal cell layer of the CA1, being lower in the pyramidal cells of CA2, and CA3 fields. High levels of hybridization were seen in dentate gyrus for PDE4A and PDE4D (Fig. 7A2). High hybridization levels for PDE4D were detected in the pyramidal cell layer of CA2 and CA3 fields and intermediate hybridization in pyramidal cell layer of CA1 (Fig. 7A5). Entorhinal cortex showed high levels of expression of both PDE4A and PDE4B mRNA (Fig. 7A2 and A3), whereas, PDE4D and PDE4C mRNAs were detectable at moderate and low levels, respectively (Fig. 7A4 and A5).

3.2.4. Thalamus

PDE4B mRNA was detected at moderate levels in ventral-lateral and ventroposterior nuclei of the thalamus (Fig. 7A3). Lower expression of PDE4C mRNA could be observed in the same nuclei (Fig. 7A4). PDE4D mRNA showed moderate levels of hybridization signal in the lateral geniculate nucleus (Fig. 7A5). PDE4B mRNA (Fig. 7A3), and PDE4C mRNA were detected with a weaker hybridization signal in this nucleus (Fig. 7A4).

3.2.5. Cerebellum

The cerebellar cortex showed relatively strong hybridization signals for PDE4A, PDE4B, PDE4C and PDE4D in the granule cell layer of the cerebellum (Fig. 7B2–B5). In the cerebellar nuclei, PDE4A was present at low levels (Fig. 7B2), PDE4B at high, specially in the lateral, interpositus and at lower levels in the fastigial nucleus and PDE4D was also present, mostly in the lateral nucleus (Fig. 7B3 and B5). PDE4B mRNA was the only isozyme that showed high levels of specific hybridization in white matter (Fig. 7B3).

3.3. Distribution of PDE4 isozyme mRNAs and [^{3}H]rolipram binding sites in rat brain

Abundant levels of PDE4A, PDE4B and PDE4D mRNAs expression were detected in different neuronal populations in many brain areas. On the contrary, hybridization signal for PDE4C mRNA was detected exclusively in the internal plexiform and internal granular layers of the olfactory bulb (not shown). Although PDE4B mRNA expression was most conspicuous in

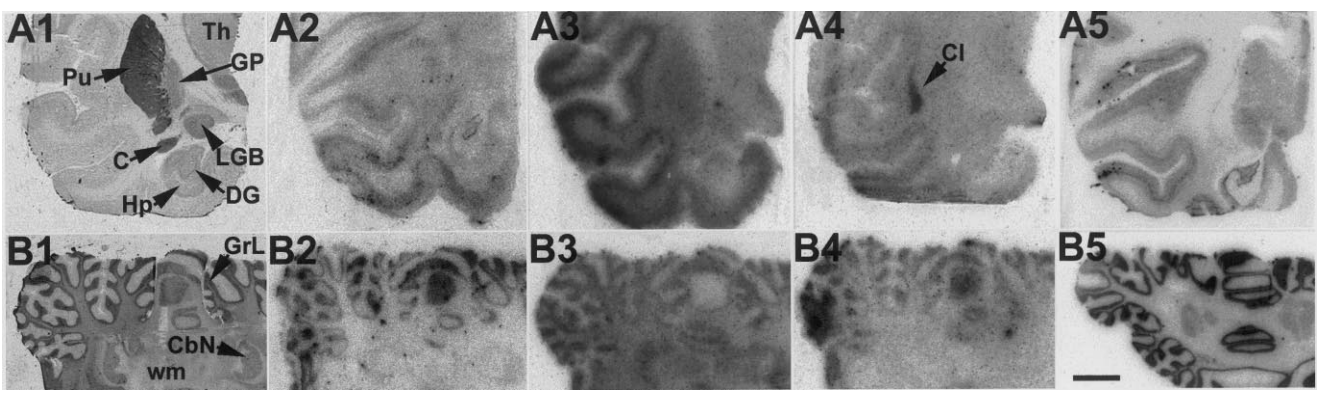

Fig. 7. Comparison of the distribution of PDE4 isozyme mRNA determined by in situ hybridization in several regions of the monkey brain. Pictures are digital photographs from film autoradiograms. A1–B1 are consecutive sections to A3–B3 stained for acetylcholinesterase activity. A2–B2, PDE4A mRNA; A3–B3, PDE4B mRNA; A4–B4, PDE4C mRNA; A5–B5, PDE4D mRNA. Note the high levels of signal for PDE4B mRNA in the putamen and in white matter and the high intensity of PDE4C labeling in the claustrum. Bar: 5 mm.

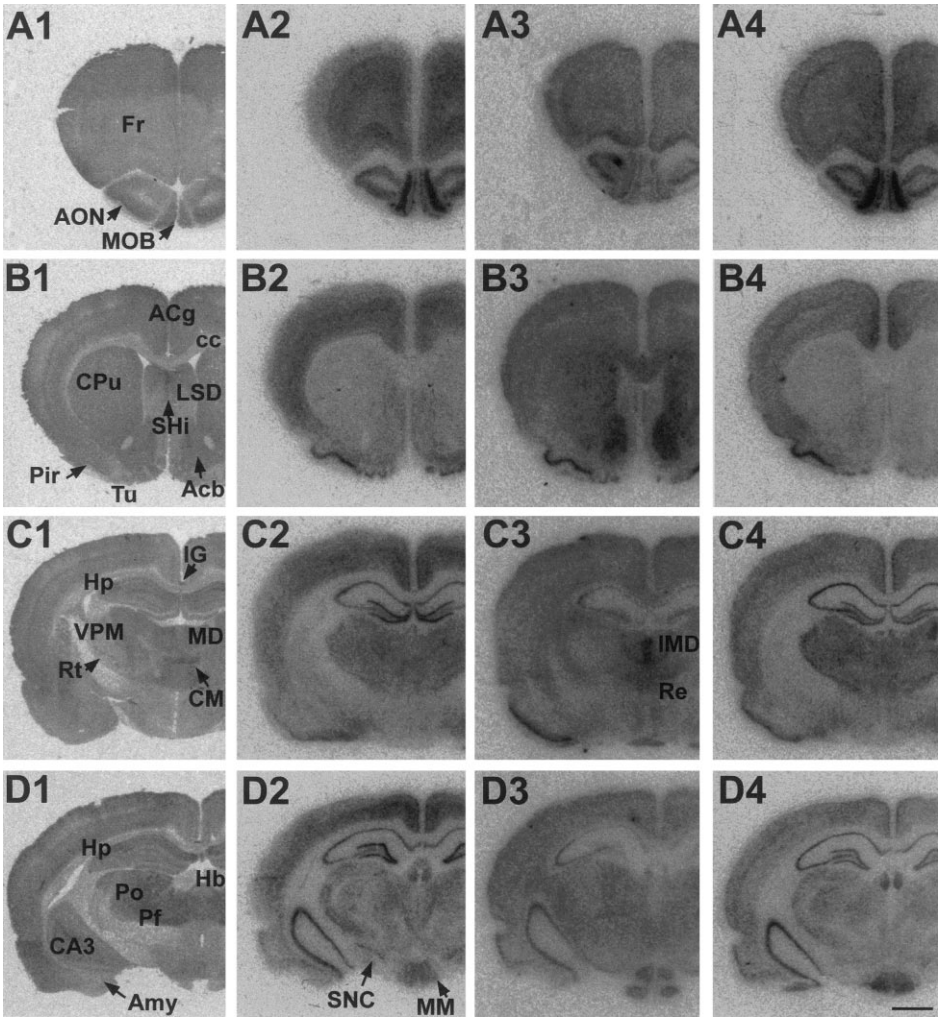

Fig. 8. Regional distribution of [^{3}H]rolipram binding and several PDE4 isozyme mRNAs in consecutive sections of the rat brain at different rostrocaudal levels. A1–H1, [^{3}H]rolipram [2 nM]. Autoradiographic images of PDE4A mRNA (A2–H2), PDE4B mRNA (A3–H3) and PDE4D mRNA (A4–H4) visualized by in situ hybridization with the corresponding labeled oligonucleotide. Pictures are digital photographs from film autoradiograms. Bar: 2 mm.

neurons, it was also detected in non-neuronal cells in many fiber tracts throughout the brain. Glial cells presented moderate levels of PDE4B mRNA.

3.3.1. Cerebral cortex

The parietal cortex showed high levels of PDE4A mRNA (layers V and VI), PDE4D mRNA (layers IV and deep part of VI), and PDE4B mRNA (layers II–III) and [^{3}H]rolipram binding sites (layers II–III). The cinguiate cortex presented high expression levels of PDE4D mRNA, mainly in layer II–III, (Fig. 8B4) moderate levels of PDE4A mRNA expression in layer V (Fig. 8B2), and low levels of PDE4B mRNA in layer II–III. Few PDE4B mRNA labeled cells were also detected in layer I (Fig. 8B3). High densities of [^{3}H]rolipram binding sites were seen in the cingulate cortex with a homogeneous labeling in all the layers (Fig. 8B1). In the retrosplenial cortex, both PDE4D and PDE4A mRNAs showed high expression levels, with PDE4D mRNA being present in layer II–III and PDE4A mRNA in layer V (Fig. 8E4 and E2, respectively). Low levels of PDE4B mRNA transcripts were detected in layer II–III (Fig. 8E3). Low to moderate densities of [^{3}H]rolipram binding sites were also found in this area (Fig. 8E1).

3.3.2. Olfactory system

In the anterior olfactory nucleus, high levels of both PDE4A (Fig. 8A2) and PDE4D mRNA (Fig. 8A4) were present in all the different parts of this nucleus; external, lateral, dorsal, medial and ventroposterior part, whereas, intermediate levels of mRNA coding for PDE4B were observed (Fig. 8A3). Binding sites for [^{3}H]rolipram were also visualized in this brain area (Fig. 8A1).

The main olfactory nucleus presented a laminar distribution of PDE4A, PDE4B and PDE4D mRNAs. High levels of both PDE4A (Fig. 9B) and PDE4D

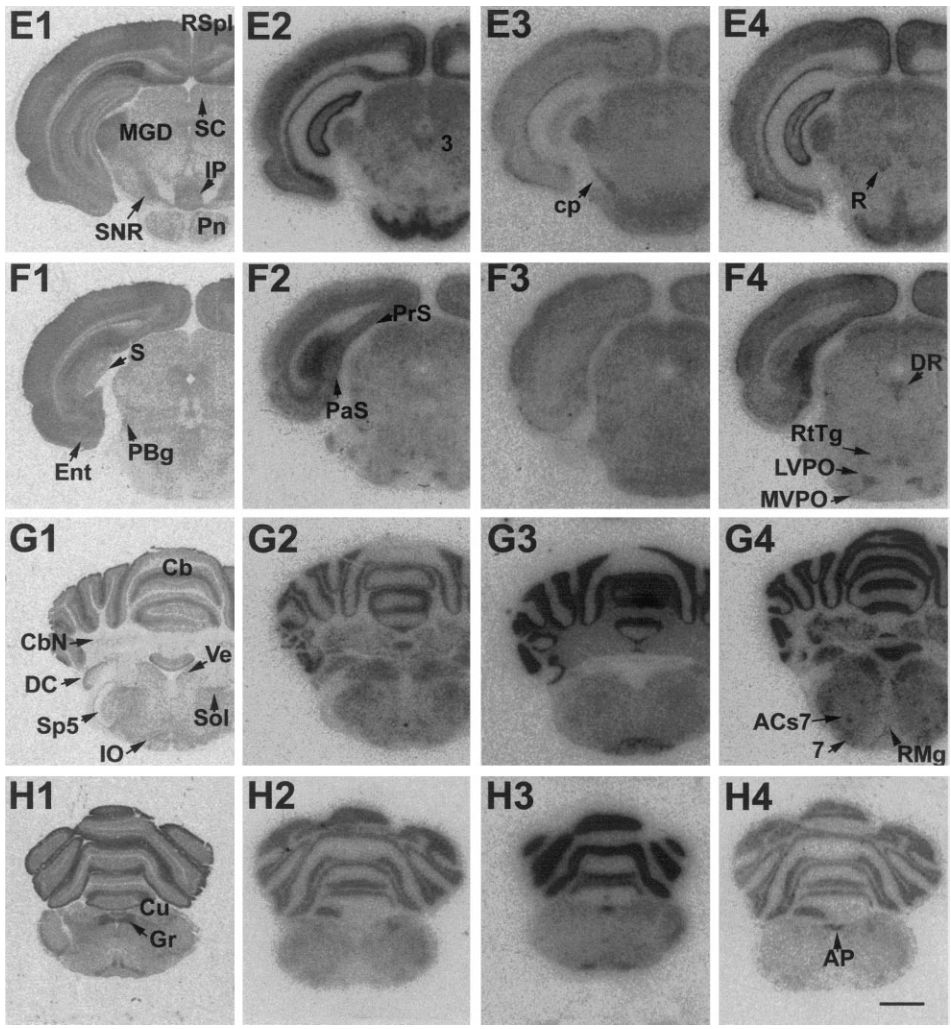

Fig. 8. (*Continued*)

mRNA (Fig. 9D) were detected in the glomerular layer of the olfactory nucleus, close to the olfactory nerve, with PDE4B mRNA being expressed at moderate levels (Fig. 9C). High levels of PDE4A and PDE4D mRNAs were also observed in the mitral cell layer, including the sublayer of middle tufted cells, as well as in both external and internal plexiform layers, whereas, PDE4B mRNA expression was moderate. The densest accumulations of PDE4A and PDE4D mRNAs were found in the internal granule cell layer. Few PDE4B mRNA labeled cells were present in this layer. [^{3}H]rolipram binding sites (Fig. 8A1) were visualized in the main olfactory nucleus, the highest densities being found in the internal granule cell layer.

Strong hybridization signals for PDE4A, PDE4B and PDE4D mRNAs were observed in the dense pyramidal cell layer (layer II) of the piriform cortex (Fig. 8B2–B4), in contrast, low binding site densities were visualized with [^{3}H]rolipram (Fig. 8B1).

Intermediate levels of mRNA coding for PDE4A and PDE4B were present in the olfactory tubercle (Fig. 8B2 and B3); the highest levels were detected in the dense cell layer, and moderate levels in the multiform cell layer. In both layers PDE4D mRNA expression was low (Fig. 8B4). Intermediate to low densities of [^{3}H]rolipram binding sites were found in the olfactory tubercle (Fig. 8B1).

Intermediate levels of PDE4A mRNA and low levels of PDE4D mRNA were present in the granule cell clusters of the islands of Calleja. PDE4B mRNA was often seen on the external borders of cells clusters, whereas, labeled cells inside the clusters could be occasionally observed. A similar distribution pattern appeared in the insula magna.

3.3.3. Basal ganglia and related areas

The highest hybridization signal observed corresponded to PDE4B mRNA in the nucleus accumbens, being the labeled cells more numerous in the shell pole than in the core pole. The caudate-putamen presented high levels of PDE4B mRNA expression (Fig. 8B3), mostly in the dorsolateral part and presenting a patchy

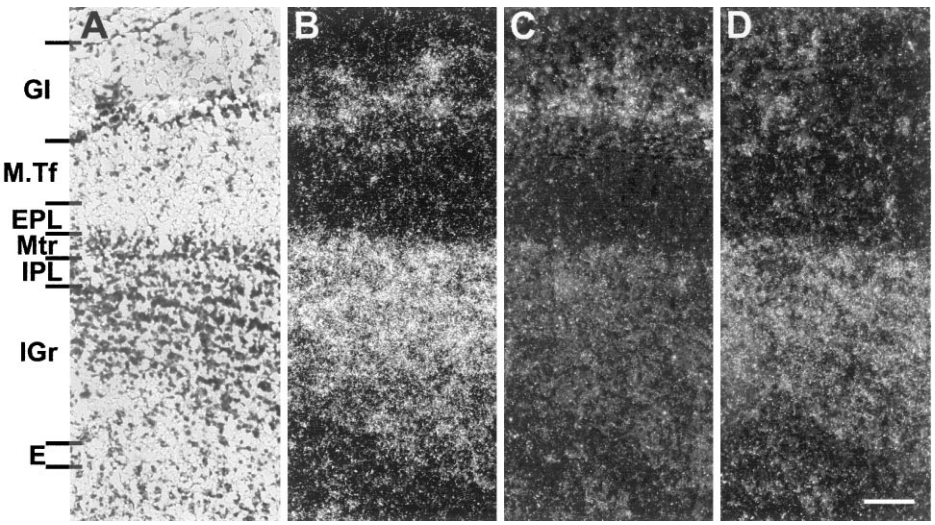

Fig. 9. Cellular localization of several PDE4 mRNA in serial coronal sections of the rat main olfactory bulb. Autoradiographic images are presented as darkfield photomicrographs from emulsion-dipped tissue sections in which autoradiographic grains are seen as bright points. (A) bright-field photomicrograph from a consecutive section to B–D stained with cresyl violet. (B) PDE4A mRNA. (C) PDE4B mRNA. (D) PDE4D mRNA. Bar: 1 mm.

distribution. Low hybridization signals for PDE4A and PDE4D mRNAs were detected in the accumbens nucleus and caudate-putamen (Fig. 8B2 and B4). PDE4B mRNA densities were high in corpus callosum and low in the anterior commissure (Fig. 8B3). In the genus corpus callossum, low densities of binding sites of [^{3}H]rolipram were detectable in comparison with the high densities observed in the accumbens nucleus and caudate-putamen, without apparent gradient in both striatal areas (Fig. 8B1).

Intermediate levels of hybridization for PDE4D mRNA were seen in spaced and small cells of the substantia nigra pars reticulata, and pars compacta (Fig. 8D4 and E4). PDE4A mRNA was mainly observed in the pyramidal and fusiform cells of the pars compacta and in the medium and large ovoid cells of the pars reticulata (Fig. 8D2 and E2). No specific hybridization signal of PDE4B mRNA was detectable in the substantia nigra (Fig. 8D3 and E3). Moderate densities of [^{3}H]rolipram binding sites were localized in pars reticulata, although lower concentrations were found in pars compacta (Fig. 8E1 and D1).

3.3.4. Septum and hippocampal formation

PDE4A mRNA presented a homogeneous distribution at intermediate densities in the lateral septum. Labeled cells were seen in the ventral part (type III neurons), in the dorsal part (type I) and at high levels in the intermediate part (type IIb neurons), PDE4A mRNA was detectable in the large cells of the medial septum and in the vertical limb of the diagonal band (Fig. 8B2). Strongly labeled cells were also seen in the septohippocampal nucleus. PDE4B mRNA showed a similar distribution to PDE4A mRNA but at lower expression levels (Fig. 8B3). PDE4D mRNA was detected in the lateral septal nucleus in type I neurons of the dorsal part (Fig. 8B4). Few labeled cells were also observed in type I neurons of the vertical limb of the diagonal band, as well as in the septohippocampal nucleus. High densities of [^{3}H]rolipram binding sites were also found in the lateral septum, particularly in its dorsal part (Fig. 8B1).

All three PDE4 mRNAs were highly expressed in the pyramidal cell layer of the CA2, whereas, in CA1 and CA3 expression of PDE4A and PDE4D was intermediate to high and very low for PDE4B. The granule cell layer of the dentate gyrus contained intermediate to high levels of PDE4A and PDE4D and no expression of PDE4B, whereas, polymorphic cells presented intermediate levels for PDE4D and low for PDE4A and PDE4B mRNA (Fig. 8 panels C and D and Fig. 10B–D). In the pyramidal cell layer of the subiculum and in layers II and III of the pre- and para-subiculum, moderate to high levels of mRNA expression was observed for the three isoforms (Fig. 8F2–F4). In the indusium griseum, few labeled cells were seen for PDE4A, PDE4B and PDE4D.

High densities of [^{3}H]rolipram binding sites were detected in the entire hippocampus, specially in the pyramidal cell layer of the CA1 (Fig. 8C1 and D1 and Fig. 10A). Moderate densities were visualized in pyramidal cells layer of CA2, CA3, in both, granule and polymorphic cell layer of the dentate gyrus and in the stratum lacunosum-moleculare. Lower binding site densities were present in the stratum oriens and stratum radiatum (Fig. 10A). High densities were also detected in the pyramidal cell layer of the subiculum, including the pre- and parasubiculum, mostly in their layers II

and III (Fig. 8F1) and in the indusium griseum (Fig. 8C1).

In the entorhinal cortex, moderate levels of PDE4A mRNA were detected in layers II and V (Fig. 8F2), high PDE4D mRNA levels in layers II and III and moderate to low levels of PDE4B mRNA in layer II (Fig. 8F4 and F3, respectively).

The different nuclei of the amygdala showed differential expression for the three PDE4 isozymes. High levels of transcripts for PDE4A mRNA were observed in the amygdalopiriform transition area, in both the superficial layer 2 and the deep layer 3. Also, high transcription levels for PDE4B mRNA were visualized in the medial amygdaloid group, mainly in the anterodorsal part in the small cells of the bed nucleus of the accessory tract of the olfactory amygdala, as well as in the sublamina 1-α and in the supratangential layer of the anterior cortical nucleus. PDE4D mRNA strongly labeled cells were appreciated in the posteroventral part of the medial amygdaloid group (Table 1). In contrast, low densities of [^{3}H]rolipram binding sites were visualized in the amygdaloid complex, mainly in the medial and basolateral amydaloid nuclei, as well as in the amygdalopiriform transition area (Fig. 8D1).

3.3.5. Diencephalon

In the thalamus, the levels of PDE4A mRNA were moderate to high in the laterodorsal and ventroposterior nuclei (Fig. 8C2 and D2), and lower in the mediodorsal, parafascicular, lateroposterior and reticular thalamic nuclei. PDE4B mRNA was present at very high hybridization levels in many intralaminar nuclei, such as centromedial, centrolateral, intermediodorsal, and reuniens, whereas, moderate levels were seen in the parafascicular thalamic nucleus (Fig. 8C3 and D3). The levels of PDE4D mRNA were high in the ventroposterior nucleus (Fig. 8C4 and D4) and moderate in the nuclei of the posterior thalamus group, as well as in the parafascicular and laterodorsal thalamic nuclei. Strong hybridization signals for PDE4A, PDE4D and moderate for PDE4B mRNAs were detected in the medial and lateral habenular nucleus (Fig. 8C2–C4 and Fig. 11C–E). Both PDE4A and PDE4D mRNA showed intermediate levels of hybridization in the lateral geniculate nucleus (ventral and dorsal pars), PDE4D mRNA levels were high in the medial geniculate nucleus (Fig. 8E4), where PDE4A mRNA and PDE4B mRNA were present at intermediate levels (Fig. 8E2 and E3). Moderate densities of bound [^{3}H]rolipram were found in many thalamic nuclei, such as the mediodorsal and ventroposterior nuclei (Fig. 8C1 and D1), with higher densities in the laterodorsal and lateroposterior nuclei, as well as in the posterior and the parafascicular thalamic nuclei. High densities of binding were also localized in the medial and dorsal geniculate nucleus (Fig. 8E1). Low levels of binding sites were visualized over the habenular nuclei (Fig. 8D1 and Fig. 11 B). In addition, moderate levels of both PDE4A and PDE4D mRNA were found in the zona incerta, although lower levels of PDE4B mRNA and [^{3}H]rolipram binding sites were detected in this region (Table 1).

In the hypothalamus, (Fig. 8D2 and D4) both PDE4A and PDE4D mRNA transcripts were present at high levels in the medial mammillary nucleus. High

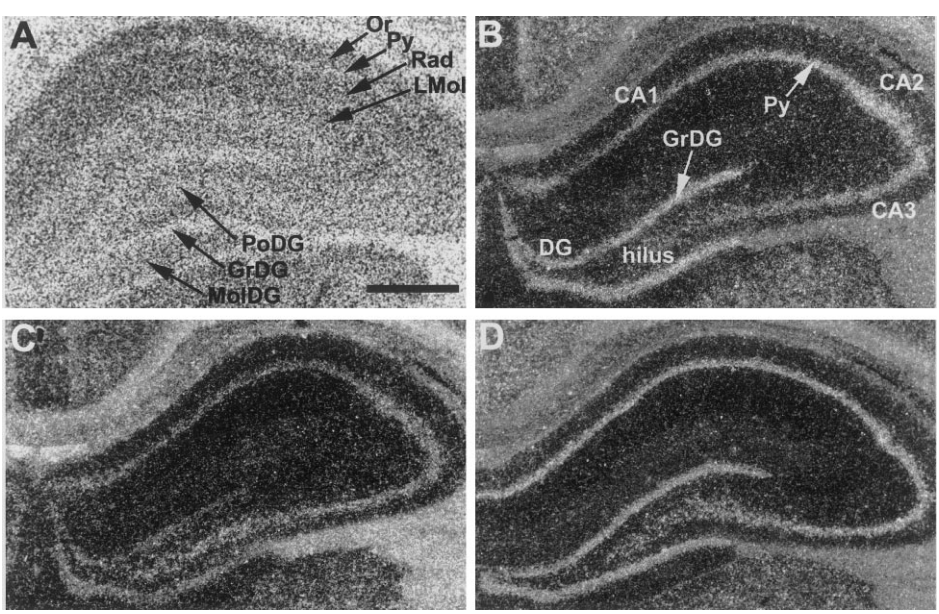

Fig. 10. Distribution of [^{3}H]rolipram binding sites and PDE4 mRNAs in serial coronal sections through the rat hippocampal formation. A is a bright-field photomicrograph from a film autoradiogram showing the [^{3}H]rolipram binding sites. B, C and D are dark-field photomicrographs from emulsion-dipped tissue. B; PDE4A mRNA. C; PDE4B mRNA. D; PDE4D mRNA. Note the lack of detectable hybridization signal for PDE4B mRNA in the dentate gyrus. The different layers of the hippocampus are indicated in panel A. Bar; 0.5 mm.

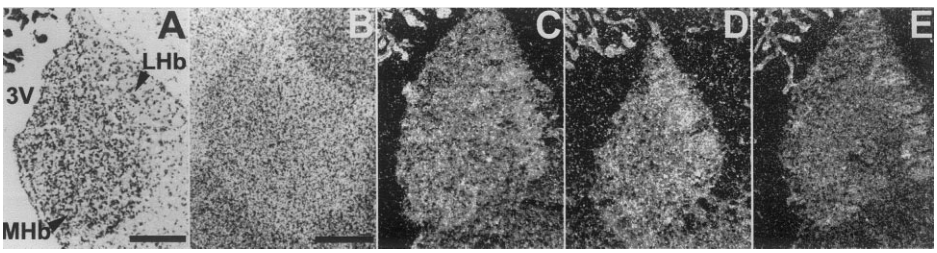

Fig. 11. Distribution of [^{3}H]rolipram binding sites and PDE4 mRNAs in the rat habenula. A is a bright-field photomicrograph from a consecutive section to C stained with cresyl violet. B is a bright-field photomicrograph from a film autoradiogram showing the [^{3}H]rolipram binding sites. C, D and E are dark-field photomicrographs from emulsion-dipped tissue. C; PDE4A mRNA. D; PDE4B mRNA. E; PDE4D mRNA. Note the high density of grains in the lateral habenular nucleus for all the mRNAs. Bar in A (A = C = D = E); 150 μm. Bar in B; 250 μm.

levels of PDE4A mRNA were detected in the supramammillary nucleus, and lower levels in the lateral mammillary nucleus. In contrast, few -PDE4D mRNA labeled cells were detected in the lateral mammillary nucleus, whereas, strongly labeled cells were observed in the supramammillary nucleus. Intermediate levels of mRNA for PDE4B were only found in the medial mammillary nucleus (Fig. 8D3). High densities of [^{3}H]rolipram binding sites were seen in both medial and lateral mammillary nucleus and low densities in the supramammillary nucleus (Fig. 8D1).

PDE4A mRNA showed few strongly labeled cells in the periventricular hypothalamic nucleus. Low levels of PDE4A and PDE4D transcripts were seen in the ventromedial and posterior hypothalamic nuclei as well as in the polymorphic cells of the arcuate nucleus, specifically in the dorsal and lateral part. PDE4B mRNA was detected in the dorsomedial, central and lateral part of the ventromedial hypothalamic nuclei and in the dorsal part of the dorsomedial hypothalamic nucleus. Low densities of [^{3}H]rolipram binding sites were visualized in the dorsomedial and ventromedial hypothalamic nucleus and in the medial-posterior part the arcuate hypothalamic nucleus.

3.3.6. Brainstem

Many nuclei of the brainstem were enriched in mRNA transcripts of the three isozymes, as summarized in Table 1. It is worth to notice the high expression of PDE4A and PDE4D mRNA in the pontine nuclei, the different parts of the interpenduncular nucleus (Fig. 8E2, E4, F2 and F4) and in the reticulotegmental nucleus of the pons. High levels of PDE4A mRNA were detected in the pedunculopontine and ventral tegmental nuclei. Moderate levels of PDE4B mRNA were seen in the cerebral peduncle and pontine nuclei (Fig. 8E3). Few labeled cells for PDE4B mRNA were seen in the lateral and caudal pars of the interpeduncular nucleus. In contrast, the pons showed only very low densities of specifically bound [^{3}H]rolipram, with the highest densities being found in the interpeduncular nucleus (Fig. 8E1).

Intermediate to high levels of PDE4D mRNA were seen in the giant and large neurons of the red nucleus and low levels in the medium size cells of this nucleus (Fig. 8E4). No signal for both PDE4A and PDE4B mRNA was detected in this nucleus. Intermediate levels of PDE4D mRNA were seen in the ventromedial and dorsomedial part of the dorsal raphe nuclei (Fig. 8F4), being both PDE4A and PDE4B mRNAs undetectable. Low levels of PDE4D mRNA were detected in the raphe magnus (Fig. 8E4). No hybridization signals of any PDE4 isozymes were seen neither in the raphe pallidus nor in the raphe obscurus. Very low [^{3}H]rolipram binding site densities were observed in the dorsal raphe nucleus and in the red nuclei (Fig. 8F1 and E1).

High levels of PDE4B mRNA were found in the pineal gland, whereas, no hybridization signals of both PDE4A and PDE4D mRNA neither [^{3}H]rolipram binding were detected in this gland (Table 1).

In the superior colliculus, PDE4D mRNA was present at high levels, specially in the superior gray layer (Fig. 8E4), PDE4A mRNA was detected at moderate levels in the superior gray layer, as well as in the intermediate gray and white layer (Fig. 8E2) and PDE4B mRNA was visualized at moderate levels in the optical layer and superior gray layer, and at lower levels in the intermediate white layer (Fig. 8E3). [^{3}H]rolipram binding sites were detected at low densities with no apparent differences among the layers (Fig. 8E1).

Intermediate levels of PDE4A, PDE4B and PDE4D mRNA were found in the middle subdivision of the parabigeminal nucleus (Fig. 8F2–F4). Similarly, intermediate binding site densities of [^{3}H]rolipram were visuallized in this area (Fig. 8F1).

PDE4B mRNA was detected at very high levels in the inferior olivary complex, in the dorsal and principal accessory olive, as well as in the subnuclei A, B and C of the medial olivary nucleus (Fig. 8G3 and H3). The trigeminal sensory nuclei presented intermediate to high levels of PDE4A, PDE4B and PDE4D mRNA, mainly in the caudal subdivision of the spinal trigeminal nucleus (including oral, dorsal and ventral part), as well as

in layers II and III of the caudal subdivision of this nucleus (Fig. 8G2–G4 and H2–H4). In addition, moderate levels of PDE4B mRNA were detected in the spinal trigeminal tract (Fig. 8G3 and H3).

The part parvocellular and magnocellular of the medial vestibular nucleus contained high hybridization levels of PDE4D mRNA (Fig. 8G4), moderate levels of PDE4A mRNA (Fig. 8G2) and a few PDE4B mRNA labeled cells (Fig. 8G3) The spinal vestibular nucleus presented high contents of PDE4D mRNA, moderate for PDE4A mRNA and low for PDE4B mRNA. The central part of the dorsal cochlear nuclei (Fig. 8G4) presented high expression levels of PDE4D mRNA, moderate levels of PDE4A mRNA (Fig. 8G2) and low of PDE4B mRNA (Fig. 8G3). The cuneate and gracile nuclei presented moderate levels of hybridization for both PDE4A and PDE4D mRNA (Fig. 8H2 and H4) and low for PDE4B mRNA (Fig. 8H3). The nucleus of the solitary tract contained moderate levels of PDE4A mRNA and low of PDE4B mRNA (Fig. 8G2 and G3). Strongly labeled cells for PDE4A mRNA were seen in the principal oculomotor nucleus, including the parvicellular part and the supraoculomotor periaqueduct (Fig. 8E2), whereas, a few PDE4D mRNA labeled cells could be observed (Fig. 8E4). The ependymal cells of the area postrema presented high hybridization signal for PDE4D mRNA (Fig. 8H4) and intermediate signal for PDE4B mRNA (Fig. 8H3).

High densities of [^{3}H]rolipram binding sites were localized in the nucleus of the solitary tract and in the inferior olivary complex (Fig. 8G1). Moderate densities were found in the dorsal cochlear, mainly in the first (molecular) layer (Fig. 8G1), gracile and cuneate nuclei, as well as in the area postrema (Fig. 8H1). Lower binding site densities were detected in the spinal trigeminal nucleus, and in the medial, spinal and lateral vestibular nuclei (Fig. 8G1).

3.3.7. Cerebellum

The granule cell layer of the cerebellum showed very strong hybridization signals for PDE4B and PDE4D mRNAs, and moderate levels of PDE4A mRNA and [^{3}H]rolipram binding sites (Fig. 8G2–G4, H2–H4 and Fig. 12B–D). Moderate to high levels of PDE4B mRNA were also detected in the white matter of the cerebellum (Fig. 12C). In contrast, the molecular layer only presented high densities of [^{3}H]rolipram binding sites (Fig. 12A). No hybridization signals of any of the

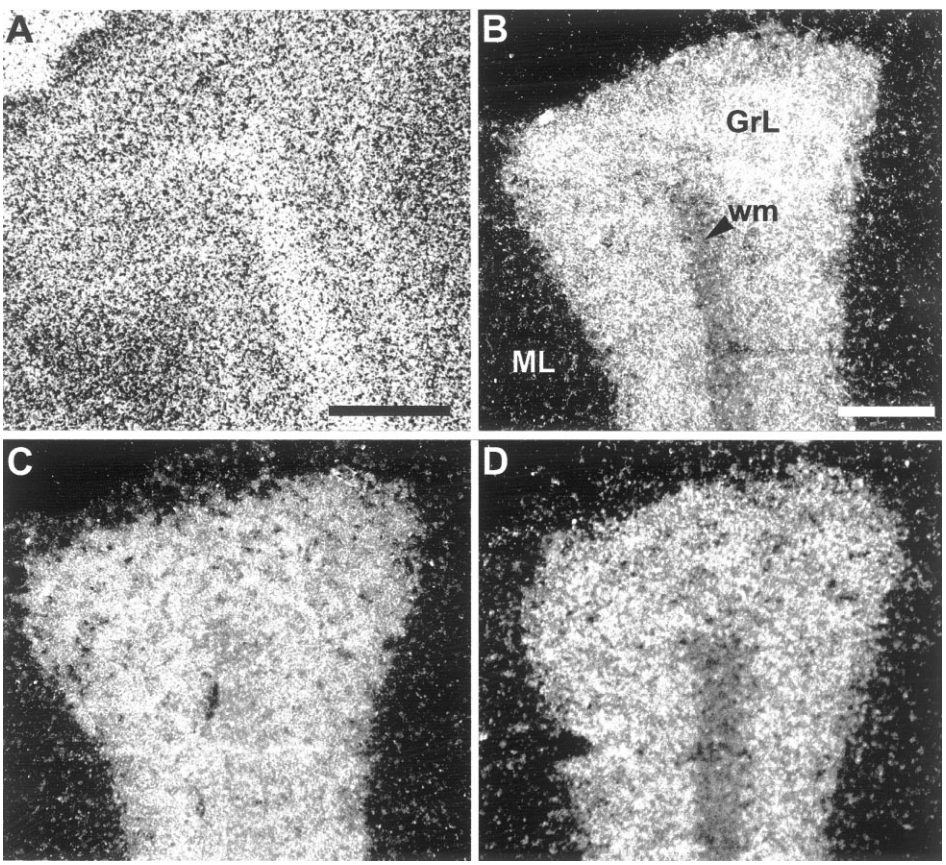

Fig. 12. Distribution of [^{3}H]rolipram binding sites and PDE4 mRNAs in the rat cerebellum in serial sections. A is a bright-field photomicrograph from a film autoradiogram showing the [^{3}H]rolipram binding sites. B, C and D are dark-field photomicrographs from emulsion-dipped tissue. B; PDE4A mRNA. C; PDE4B mRNA. D; PDE4D mRNA. Note the high density of binding sites in the molecular layer. Note the presence of PDE4B mRNA in the white matter. Bar in A; 250 μm. Bar in B (B = C = D); 200 μm.

four PDE4 isozymes could be appreciated in the Purkinje cell layer. Several cerebellar nuclei contained high hybridization levels of PDE4D mRNA (dentate, fastigial and intermediate), and moderate for PDE4A mRNA (interpositus, lateral parvicellular and lateral dentate) Fig. 8G4 and 8G2, respectively. Lower binding site densities of [^{3}H]rolipram were detected in the deep cerebellar nuclei.

4. Discussion

By using oligonucleotide probes that selectively recognize the transcripts of the four isozyme forms of the PDE4 family (PDE4A, PDE4B, PDE4C and PDE4D), we have examined their regional distribution and compared them in the brain of human, monkey and rat. Our results show that in the brain of these three species, PDE4A, PDE4B and PDE4D mRNA expression is abundant and widely distributed, not only in neuronal cells but also in white matter cells, especially PDE4B and PDE4D. An important finding is the presence of PDE4C mRNA in some brain structures in both human and monkey, contrasting with the restricted expression of this mRNA in the rat brain, where it is found exclusively in olfactory bulb. In parallel, and by using the PDE4-specific inhibitor [^{3}H]rolipram, we have visualized the binding sites in the brain of the three species. To our knowledge, this is the first detailed report of the distribution of the four PDE4 isozymes in human and monkey. Earlier studies have only partially addressed this issue using Northern blot and RT–PCR assays.

4.1. PDE4 mRNAs distribution in human brain

We have found that in human brain, the four PDE4 isozyme mRNAs presented a differential pattern of expression at both regional and cellular level. PDE4B and PDE4D were the most abundant isoforms found in human brain followed by PDE4A. In contrast, PDE4C appeared to be a minor isoform present only in areas of the brain such as cerebral cortex, few thalamic nuclei and cerebellum. Earlier studies have shown the presence of PDE4C mRNA by Northern blot analyses (Engels et al., 1995b; Obernolte et al., 1997) and RT–PCR (Engels et al., 1994) in RNA from total human brain. In fact, PDE4C isozyme cDNA was isolated from a cDNA library from human substantia nigra (Engels et al., 1995b). We did not detect in our in situ hybridization experiments, the presence of PDE4C mRNA in human substantia nigra.

We have studied the cellular expression for the four isozymes in different human brain areas; cortex, basal ganglia, limbic system, thalamus, pons-medulla, spinal cord and cerebellum. There are no other reports on the regional and cellular distribution of the PDE4 isoforms in human brain. The presence of PDE4A mRNA in total human brain has been shown by RT–PCR analysis (Engels et al., 1994) and by Northern blot analysis (Owens et al., 1997) in areas such as thalamus, hypothalamus and substantia nigra.

The results presented here show a differential regional distribution in the human brain of the mRNAs coding for the four PDE4 isozymes in neuronal and non-neuronal cells. It is worth to notice the expression of PDE4C in cortex and cerebellum, the predominance of PDE4B in basal ganglia and white matter tracts, and the presence of PDE4A, PDE4B and PDE4D in the hippocampal formation. In some tissue sections, where pia matter was present, these aforementioned isozyme mRNAs were detected. Their presence in cell types such as ependymal cells and blood vessels cannot be excluded.

4.2. PDE4 mRNAs distribution in monkey brain

In the few regions analyzed, the distribution of PDE4 transcripts was very similar to that observed in human brain. For example, the presence of PDE4A in cortex and hippocampus but not in putamen, the enrichment of PDE4B in cortex, basal ganglia and white matter tracts and of PDE4D in cortex and hippocampus, as well as the presence of PDE4C in cortex and cerebellum. All four isozymes were expressed in cerebellum, and especially in granule cells. In addition, PDE4C mRNA was found in claustrum at very high expression levels.

4.3. PDE4 mRNAs distribution in rat brain

In agreement with earlier literature (Engels et al., 1995a), the expression of PDE4C was exclusively found in the olfactory bulb. The other three isozymes were very abundant in the rat brain, especially, in the anterior brain, cortex and olfactory bulb. There were, however, some regions where they showed a distinct expression pattern, including areas such as the nucleus accumbens, hippocampal formation, pontine nuclei, raphe nuclei, inferior olive, area postrema, deep cerebellar nuclei and spinal cord. PDE4A, PDE4B and PDE4D showed a neuronal distribution in all brain areas examined. In addition, PDE4B mRNA was also present in white matter tracts.

PDE4D and PDE4A mRNA showed, in general, a widespread and similar distribution in rat brain, with few exceptions. For example and in agreement with earlier studies (Iwahashi et al., 1996), PDE4A mRNA was predominantly expressed in many nuclei of the septum, whereas, PDE4D mRNA could be detected only in the lateral septum. In contrast, PDE4D was the major isoform in brainstem nuclei such as facial nu-

cleus, cerebellar nuclei or area postrema, where PDE4B mRNA was also detected but at lower levels. The pattern of expression observed in the area postrema does not agree with the results reported by Iwahashi et al. (1996), since they also detected PDE4A mRNA in this area.

4.4. Species differences in PDE4 isoforms distribution

The regional expression of three most abundant PDE4 isoforms in a wide variety of neuronal cell types (4A, 4B and 4D) in the rat brain was very similar to that observed in human brain. There were some differences in areas such as hippocampus and cerebellum and the shared characteristic localization of PDE4B in white matter tracts. The most remarkable difference was the expression pattern of PDE4C mRNA. In human and monkey, it was found at intermediate levels in several cortical areas and cerebellum, and at higher levels, in the monkey's claustrum, whereas, in the rat brain, and in agreement with earlier studies (Engels et al., 1995a), PDE4C mRNA expression was restricted to the olfactory bulb.

PDE4A mRNA showed important differences among the three species. In rat brain, PDE4A mRNA was found at moderate levels in several brainstem nuclei, as earlier described by Iwahashi et al. (1996). However, no hybridization signal of PDE4A mRNA could be detected in the human brainstem nuclei, except in the pontine nucleus.

PDE4D mRNA was the only PDE4 isozyme expressed in the rat raphe nuclei, in contrast with the results described by Iwahashi et al. (1996), who reported expression of PDE4A and PDE4B mRNA in this nuclei. Nevertheless and in agreement with Iwahashi et al. (1996), high levels of PDE4D mRNA were also visualized in the interpeduncular nucleus, the superior colliculus and the reticulotegmental nucleus of the pons. No PDE4D mRNA was detected in these nuclei in the human brain.

The particular distribution pattern of PDE4B transcript in many fiber tracts and neurons was highly conserved among the different species studied. PDE4B mRNA distribution in rat and human brain showed, however, some differences. PDE4B mRNA was visualized in hypoglossal nucleus, cerebellar nuclei and Purkinje cells of the human brain. However, in accordance with earlier studies (Iwahashi et al., 1996), no PDE4B mRNA was present in these rat brain regions.

4.5. Correlation between PDE4 mRNA and protein expression

There are different ways to study the protein expression of the PDEs. One consists in measuring the enzymatic activity (Thompson and Appleman, 1971), but this technique lacks anatomical resolution. A second way is to use the property of rolipram to bind with nanomolar affinity to the PDE4s, outside of the catalytic site, at the so-called high affinity binding site. [^{3}H]rolipram has been earlier used to visualize, by autoradiography, the regional distribution of its binding sites in rat brain (Kaulen et al., 1989). However, these first studies were limited due to the low specific activity of the radioligand available at that time. We have now used a high specific activity [^{3}H]rolipram, which generates autoradiograms with a high degree of resolution. In analyzing these autoradiograms, several factors should be taken into account. First, the quenching of the white matter (white matter tracts will generate less grain density in spite of the equal amount of bound radioactivity (Geary and Wooten, 1985). Another factor to consider is that ligand autoradiography performed in isotonic conditions (present work) allows the visualization of [^{3}H]rolipram binding sites corresponding probably to membrane bound enzyme and cytoplasmic molecules. A limitation of rolipram is that it is not isozyme specific and labels all four PDE4 forms. In the absence of selective inhibitors of the binding of rolipram to the different isozymes, it is impossible to differentiate the isozyme components of the binding of rolipram to the tissue. Nevertheless, taking into account the differential localization of the mRNAs coding for the PDE4 isoforms, our results suggest areas of the brain where the coincidence of the expression of specific isozyme mRNA and rolipram binding sites can be used to select these selective inhibitors, when available. For example, the olfactory bulb should be rich in PDE4A, PDE4C and PDE4D, whereas, the nucleus accumbens appears to be enriched in the PDE4B form which is also present exclusively in the nucleus of the inferior olive. In the hippocampus, the granule cell layer expresses PDE4A and PDE4D, being PDE4B undetected, particularly in the posterior part. Similar differences are also seen in the pyramidal cell layer of the CA1. An interesting observation is the absence of PDE4A expression in the area postrema in the rat. This could be a region to select isozyme specific inhibitors, specially if this difference is conserved among the species, due to the fact that emesis is an important, limiting side effect of PDE4 inhibitors (Horowski and Sastre-y-Hernandez, 1985). The presence of PDE4s in the area postrema points to their possible involvement in mediating this effect.

Comparison of our data on the distribution of PDE4A, PDE4B, PDE4C and PDE4D mRNA in rat brain does generally agree with the protein localization of each one of these isozymes by immunohistochemistry (Cherry and Davis, 1999) with a few exceptions. For example, PDE4B mRNA was detected at high levels in the pyramidal cell layer of the CA2 and PDE4A mRNA was also observed in the dentate gyrus but

these two regions did not show immunolabeled cells neither with anti-PDE4B nor with PDE4A antibodies. We could not detect PDE4B mRNA in rat dentate gyrus, in contrast with the immunolabeling with the anti-PDE4B antibody described in this area (Cherry and Davis, 1999). An extrinsic origin of the protein could explain this discrepancy.

Comparison of the present results on the localization of [^{3}H]rolipram binding sites with the immunohistochemical localization of the PDE4s (Cherry and Davis, 1999) reveals interesting similarities. For example, the anti-PDE4B antibody immunoreaction in the molecular layer of the cerebellum, agrees with the high densities of binding sites found in this layer (present results; Kaulen et al., 1989). In contrast, we were unable to detect any PDE4 isozyme mRNA in this layer, but expression was observed both in granule cells and in Purkinje cells, which extend their processes (axons and dendrites, respectively) into the molecular layer. Comparison of the data derived from in vitro autoradiography with in situ hybridization studies is difficult due to the fact that by in situ hybridization histochemistry the cell bodies that contain the mRNAs coding for each isozyme are detected; whereas, with receptor autoradiography, the PDE4 protein(s), could be visualized in the cell bodies as well on distal processes. In our case, comparison is further hindered, as it was mentioned before, by the failure of currently available radioligand to individually label PDE4A, PDE4B, PDE4C and PDE4D isozymes, due to the lack of specific inhibitors for each PDE4 isozyme. In general, the distribution of [^{3}H]rolipram binding sites agrees well with the summation of the distribution of the four PDE4 isoform mRNAs (our results) and with the immunolocalization of all four PDE4 isozymes (Cherry and Davis, 1999). But there are some exceptions, for example, in the olfactory tubercle, piriform cortex and in the pontine nuclei, we have detected high levels of PDE4A, PDE4B and PDE4D mRNAs. In contrast, and in agreement with earlier studies (Kaulen et al., 1989), low densities of [^{3}H]rolipram binding sites are visualized in these regions. It is tempting to speculate that at least part of the PDE4s expressed in these nuclei could be presynaptically located.

In agreement with our observation on PDE4B mRNA localization in fiber tracts, both in rat and human brain, [^{3}H]rolipram binding sites were also present in fibers in these two species, specially, when the quenching factor is taken into account. This distribution in rat brain correlated also with that of the anti-PDE4B immunoreactivity (Cherry and Davis, 1999).

The distribution of [^{3}H]rolipram binding sites in rat brain correlated, in general, with [^{3}H]cyclic-AMP binding sites described by Araki et al. (1992).

[^{3}H]cyclic-AMP binding sites distribution by membrane binding assay has been also reported in human brain (Schneider et al., 1986). In agreement with our results, these authors found high levels of binding sites in several brain regions such as frontal, occipital, temporal and parietal cortex, hippocampus and cerebellar cortex. In addition, membrane binding studies have been reported in Alzheimer's disease post-mortem brain. (Bonkale et al., 1999). Results showed an alteration of [^{3}H]cAMP binding to cytosolic but not particulate protein kinase A, in the entorhinal cortex in Alzheimer's disease brain.

4.6. PDE4 function

Overlapping expression of the four PDE4 isozymes was observed in brain regions involved in processes of learning and memory; such as the olfactory system and the hippocampus. cAMP-specific PDE4 isozymes could play an important role in processes of learning and memory. In fact, the *dunce* gene of *Drosophila melanogaster* was the first gene isolated that affected behavior (Dudai et al., 1976), flies with mutations in *dunce* are deficient in learning and memory (Davis, 1996). Biochemical analysis of brain extracts from *dunce* flies showed them to be deficient in cAMP PDE activity (Byers et al., 1981). Mammalian PDE4 cDNAs were subsequently isolated by using the *dunce* cDNA to probe mammalian cDNA libraries (Davis et al., 1989).

Rolipram is a selective cAMP phosphodiesterase type 4 inhibitor that preferentially increases cAMP levels in the brain in the absence of stimulation of neurotransmitter receptors (Schneider, 1984; Schneider et al., 1986). Most of the information available on the possible role of PDEs derives from the studies done, with rolipram and few other molecules. Rolipram can interfere with many activities of the brain cells, mood, depression, anxiety, memory. For example, the effects of rolipram administration on cellular and animal models of memory formation (Barad et al., 1998; Bach et al., 1999) have shown that amplification of signals through the cAMP pathway may lower the threshold for generating long-lasting, long-term potentiation and increase behavioral memory. Rolipram, at concentrations not affecting basal cAMP levels, increases cAMP responses in hippocampal slices to stimulation with forskolin and induces persistent longterm potentiation in CA1 after a single tetanic train (Barad et al., 1998). Rolipram treated rats exhibit some anxiolytic-like activity in the elevated plus-maze test (Silvestre et al., 1999b) which appears to be independent of the concurrent reduction in the locomotor activity. It has been also shown that rolipram induced potent and dose-dependent hypoactivity in rats (Silvestre et al., 1999a) decreasing both locomotion and rearing, effect that may be modulated by the cholinergic system. It is worth to notice the high densities of [^{3}H]rolipram binding sites present in human in the nucleus basalis of Meynert, the

area containing the cell bodies of the cholinergic neurons projecting to the neocortex and which degenerates in Alzheimer's disease brains. Further evidence for a close relationship between PDE4D and muscarinic cholinergic mechanisms has been recently shown in the lung of the knock out mice of this enzyme (Hansen et al., 2000) (see below).

Rolipram has anti-depressant effects, and it has been shown that anti-depressants modify PDE4 expression (Takahashi et al., 1999). Emesis is one of the most common side effects of PDE4 inhibitors administration. The mechanism by which PDE4 inhibition results in increased vomiting and nausea in species such as dog and human (Bertolino et al., 1988; Hebenstreit et al., 1989; Heaslip and Evans, 1995) is not fully understood, but probably includes both central and peripheral sites of actions. The presence of mRNAs coding for PDE4B and PDE4D in the area postrema, a region which is known to mediate these effects (Borinson and Wang, 1953; Carpenter et al., 1988), suggests that cAMP signaling modification in this area could mediate the emetic effects of PDE4 inhibitors.

Many other central and peripheral effects have been described after administration of PDE4 inhibitors; as anti-inflammatory and also related to their intriguing presence in white matter in multiple sclerosis and in allergic encephalitis, an animal model of multiple sclerosis (Sommer et al., 1995). There are also studies on the inhibition of LPS-induced expression of TNF-α in the rat brain (Buttini et al., 1997), on the reduction of neuronal damage following cerebral ischemia in the gerbil (Kato et al., 1995), Alzheimer's disease (McGeer et al., 1990; McGeer and McGeer, 1995) and others.

The fine tuning of intracellular levels of cAMP appears to be an important regulatory mechanism in several brain functions. It has been speculated that each PDE isozyme plays slightly different roles. The inactivation of one PDE should produce a loss of function. Flies deficient in the *D. melanogaster dunce* PDE (homologue of the mammalian PDE4D) display impairments in the central nervous system and reproductive functions (Dudai et al., 1976). Mice deficient in PDE4D exhibit delayed growth, as well as reduced viability and female fertility (Jin et al., 1999). In these knock out mice, the airways are no longer responsive to cholinergic stimulation (Hansen et al., 2000). The lung phenotype of the PDE4D-deficient mice demonstrates that this gene plays a non-redundant role in cAMP homeostasis. Elimination of a single PDE4 gene causes a significant reduction in PDE activity and an increase in resting and stimulated cAMP levels in the lung, indicating that the other PDE4s are not upregulated, thus, supporting the idea that each PDE could have unique and non-overlapping functions in cell signalling. This is an important point for the development of PDE4 isozyme-specific inhibitors as therapeutic agents.

In conclusion, our studies have demonstrated that PDE4A, PDE4B, PDE4C and PDE4D present a differential cellular distribution in human, monkey and rat brain. This suggests that the different isozymes could be associated also to distinct functions. The development of specific inhibitors for each PDE4 isozyme will allow to proof their implication in different functions. Studies with animal lesions and human neuropathologies could help to elucidate a most precise and detailed cellular localization of the expression of these isozymes. Our results had pinpoint areas in human and rat brain where these different effects could be studied.

Acknowledgements

This work was supported, by grants from Fundació La Marató de TV3 (# 1017/97), CICYT (SAF1999-0123) and CICYT (# 2FD97-0395). S.P.-T. is a recipient of a fellowship from CIRIT (Generalitat de Catalunya) and X.M. from CIRIT (Centre de Referència de la Generalitat de Catalunya).

Appendix A. Index of structures

3, oculomotor nucleus; 3V, 3rd ventricle; 4, trochlear nucleus; 6, abducens nucleus; 7, facial nucleus; 11, spinal accessory nucleus; 12, hypoglossal nucleus; ac, anterior commissure; Acb, accumbens nucleus; Acc, pars accessoria of the ventral posteromedial nucleus of the thalamus; ACg, anterior cingulate cortex; Acs7, accessory facial nucleus; Amy, amygdala; AON, anterior olfactory nucleus; AP, area postrema; B, basal nucleus of Meynert; C, caudate nucleus; CA1, CA1 field of the hippocampus; CA2, CA2 field of the hippocampus; CA3, CA3 field of the hippocampus; cAMP, cyclic adenosine 3′,5′-monophosphate; Cb, cerebellum; CbN, cerebellar nuclei; cc, corpus callossum; Ce, central thalamic nucleus; CG, central gray; Cl, claustrum; CLi, caudal linear nucleus of the raphe; CM, central medial thalamic nucleus; cp, cerebral peduncle; CPu, caudate-putamen; Cu, cuneate nucleus; DC, dorsal cochlear nuclei; De, dentate nucleus; DG, dentate, gyrus; DR, dorsal raphe nucleus; E, ependymal layer of the main olfactory bulb; Ent, entorhinal cortex; EPL, external plexiform layer of the main olfactory bulb; Fr, frontal cortex; Ge5, gelatinous layer of the caudal spinal trigeminal nucleus; GI, glomerular layer of the main olfactory bulb; GP, globus pallidus; Gr, gracile nucleus; GrDG, granule cell layer of the dentate gyrus; GrL, granular layer of the cerebellum; Hb, habenula; Hp, hippocampal formation; IG, indusium griseum; IGr, internal granule cell layer of the main olfactory bulb; IMD, intermediodorsal thalamic nucleus; IO, inferior olive; IOM, medial nucleus of the inferior olive;

IOPr, principal nucleus of the inferior olive; IP, interpeduncular nucleus; IPL, internal plexiform layer of the main olfactory bulb; LD, laterodorsal thalamic nucleus; LGB, lateral geniculate body; LHb, lateral habenular nucleus; Mol, stratum lacunosum moleculare of the hippocampus; LP, lateroposterior thalamic nucleus; LRt, lateroreticular nucleus; LSD, lateral septal nucleus, dorsal part; LVPO, lateroventral periolivary nucleus; M, medial thalamic nucleus; M.Tf, sublayer of middle tufted cells; MD, mediodorsa thalamic nucleus; MGB, medial geniculate body; MGD, medial geniculate nucleus, dorsal part; MHb, medial habenular nucleus; ML, molecular layer of the cerebellum; MM, medial mammillary nucleus, medial part; MOB, main olfactory bulb; MoDG, molecular layer of the dentate gyrus; Mtr, mitral cell layer of the main olfactory bulb; MVPO, medioventral periolivary nucleus; Or, stratum oriens of the hippocampus; PaS, parasubiculum; PBg, parabigeminal nucleus; PDE, phosphodiesterase; Pf, parafascicular thalamic nucleus; PI, inferior pulvinar thalamic nucleus; Pir, piriform cortex; PL, lateral pulvinar thalamic nucleus; PM, medial pulvinar thalamic nucleus; PN, paranigral nucleus; Pn, pontine nuclei; Po, posterior thalamic nucleus; PoDG, polymorphic cell layer of the hippocampus; Prk, Purkinje cells; PrS, presubiculum; Pu, putamen; Py, pyramidal cell layer of the hippocampus; R, red nucleus; Rad, stratum radiatum of the hippocampus; Re, reuniens thalamic nucleus; RMg, raphe magnus nucleus; RSpl, retrospenial cortex; Rt, reticular thalamic nucleus; RtTg, reticulo tegmental nucleus of the pons; S, subiculum; SC, superior colliculus; SHi, septohippocampal nucleus; SNC, substantia nigra, pars compacta; SNR, substantia nigra, pars reticulata; Sol, nucleus of the solitary tract; SO, superior olive; Sp5, spinal trigeminal nucleus; Sp5C, spinal trigeminal nucleus, caudal part; Th, thalamus; Tu, olfactory tubercle; Ve, vestibular nuclei; VPL, ventral posterolateral thalamic nucleus; VPM, ventral posteromedial thalamic nucleus; wm, white matter.

References

Albretsen, C., Haukanes, B.I., Aasland, R., Kleppe, K., 1988. Optimal conditions for hybridization with oligonucleotides: a study with myc-oncogene DNA probes. Anal. Biochem. 170, 193–202.

Araki, T., Kato, H., Kogure, K., 1992. Mapping of second messenger and rolipram receptors in mammalian brain. Brain Res. Bull. 28, 843–848.

Bach, M.E., Barad, M., Son, H., Zhuo, M., Lu, Y.F., Shih, R., Mansuy, I., Hawkins, R.D., Kandel, E.R., 1999. Age-related defects in spatial memory are correlated with defects in the late phase of hippocampal long-term potentiation in vitro and are attenuated drugs that enhance the cAMP signaling. Proc. Natl. Acad. Sci. USA 96, 5280–5285.

Barad, M., Bourtchouladze, R., Winder, D.G., Golan, H., Kandel, E., 1998. Rolipram, a type IV-specific phosphodiesterase inhibitor, facilitates the establishment of long-lasting long-term potentiation and improves memory. Proc. Natl. Acad. Sci. USA 95, 15020–15025.

Beavo, J.A., 1995. Cyclic nucleotide phosphodiesterases: functional implications of multiple isoforms. Physiol. Rev. 75, 725–748.

Bertolino, A., Crippa, D., di Dio, S., Fichte, K., Musmeci, G., Porro, V., Rapisarda, V., Sastre-y-Hernandez, M., Schratzer, M., 1988. Rolipram versus imipramine in inpatients with major, 'minor' or atypical depressive disorder: a double-blind double-dummy study aimed at testing a novel therapeutic approach. Int. Clin. Psychopharmacol. 3, 245–253.

Bolger, G., Rodgers, L., Riggs, M., 1994. Differential CNS expression of alternative mRNA isoforms of the mammalian genes encoding cAMP-specific phosphodiesterases. Gene 149, 237–244.

Bonkale, W.L., Cowburn, R.F., Ohm, T.G., Bogdanovic, N., Fastbom, J., 1999. A quantitative autoradiographic study of [^{3}H]cAMP binding to cytosolic and particulate protein kinase A in post-mortem brain staged for Alzheimer's disease neurofibrillary changes and amyloid deposits. Brain Res. 818, 383–396.

Borinson, H.L., Wang, S.C., 1953. Physiology and pharmacology of vomiting. Pharmacol. Rev. 5, 193–230.

Buttini, M., Mir, A., Appel, K., Wiederhold, K.H., Limonta, S., Gebicke-Haerter, P.J., Boddeke, H.W., 1997. Lipopolysaccharide induces expression of tumour necrosis factor alpha in rat brain: inhibition by methylprednisolone and by rolipram. Br. J. Pharmacol. 122, 1483–1489.

Byers, D., Davis, R.L., Kiger, J.A., 1981. Defect in cyclic AMP phosphodiesterase due to the dunce mutation of learning in Drosophila. Nature 289, 79–83.

Carpenter, D.O., Briggs, D.B., Knox, A.P., Strominger, N., 1988. Excitation of area postrema neurons by transmitters, peptides, and cyclic nucleotides. J. Neurophysiol. 59, 358–369.

Cherry, J.A., Davis, R.L., 1999. Cyclic AMP Phosphodiesterases are localized in regions of the mouse brain associated with reinforcement, movement and affect. J. Comp. Neurol. 407, 287–301.

Davis, R.L., 1996. Physiology and biochemistry of Drosophila learning mutants. Physiol. Rev. 76, 229–317.

Davis, R.L., Takayasu, H., Eberwine, M., Myres, J., 1989. Cloning and characterisation of mammalian homologs of the *Drosophila* dunce + gene. Proc. Natl. Acad. Sci. USA 86, 3604–3608.

Dewulf, A., 1971. Anatomy of the normal human thalamus. In: Topometry and Standardized Nomenclature. Elsevier, Amsterdam.

Dudai, Y., Jan, Y.-N., Byers, D., Quinn, W., Benzer, S., 1976. Dunce, a mutant of Drosophila deficient in learning. Proc. Natl. Acad. Sci. USA 73, 1684–1688.

Engels, P., Fitchel, K., Lübbert, H., 1994. Expression and regulation of human and rat phosphodiesterase type IV isogenes. FEBS Lett. 350, 291–295.

Engels, P., Abdel'Al, S., Hulley, P., Lübbert, H., 1995a. Brain distribution of four rat homologues of the Drosophila *Dunce* cAMP phosphodiesterase. J. Neurosci. Res. 41, 169–178.

Engels, P., Sullivan, M., Müller, T., Lübbert, H., 1995b. Molecular cloning and functional expression in yeast of a human cAMP-specific phosphodiesterase subtype (PDE IV-C). FEBS Lett. 358, 305–310.

Fawcett, L., Bazendale, R., Stacey, P., McGrouther, C., Harrow, I., Soderling, S., Hetman, J., Beavo, J.A., Phillips, S.C., 2000. Molecular cloning and characterization of a distinct human phosphodiesterase gene family: PDE11A. Proc. Natl. Acad. Sci. USA 97, 3702–3707.

Geary, W.A., II, Wooten, G.F., 1985. Regional tritium quenching in quantitative autoradiography of the central nervous system. Brain Res. 336, 334–336.

Hansen, G., Jin, S.-L. C., Umetsu, D.L., Conti, M., 2000. Absence of muscarinic cholinergic airway responses in mice deficient in the cyclic nucleotide phosphodiesterase PDE4D. Proc. Natl. Acad. Sci. USA 97, 6751–6756.

Heaslip, R.J., Evans, D.Y., 1995. Emetic, central nervous system, and pulmonary activities of rolipram in the dog. Eur. J. Pharmacol. 286, 281–290.

Hebenstreit, G.F., Fellerer, K., Fichte, K., Fischer, G., Geyer, N., Meya, U., Sastre-y-Hernandez, M., Schony, W., Schratzer, M., Soukop, W., Trampitsch, E., Varosanec, S., Zawada, E., Zochling, R., 1989. Rolipram in major depressive disorder: results of a double-blind comparative study with imipramine. Pharmacopsychiatry 22, 156–160.

Horowski, R., Sastre-y-Hernandez, M., 1985. Clinical effects of the neurotropic selective cAMP phosphodiesterase inhibitor rolipram in depressed patients: global evaluation of the preliminary reports. Curr. Ther. Res. 38, 23–29.

Houslay, M.D., Sullivan, M., Bolger, G.B., 1998. The multienzyme PDE4 cyclic adenosine monophosphate-specific phosphodiesterase family: intracellular targeting, regulation, and selective inhibition by compounds exerting anti-inflammatory and anti-depressant actions. Adv. Pharmacol. 44, 225–342.

Iwahashi, Y., Furuyama, T., Tano, Y., Ishimoto, I., Shimomura, Y., Inagaki, S., 1996. Differential distribution of mRNA encoding cAMP-specific phosphodiesterase isoforms in the rat brain. Mol. Brain Res. 38, 14–24.

Jin, S.-L. C., Richard, F.J., Kuo, W.-P., D'Ercole, A.J., Conti, M., 1999. Impaired growth and fertility of cAMP-specific phosphodiesterase PDE4D-deficient mice. Proc. Natl. Acad. Sci. USA 96, 11998–12003.

Kandel, E.R., Schwartz, J.H., 1982. Molecular biology of learning: modulation of transmitter release. Science 218, 433–443.

Karnovsky, M.J., Roots, I., 1964. A 'direct coloring' thiocholine method for cholinesterases. J. Histochem. Cytochem. 12, 219–221.

Kato, H., Araki, T., ltoyama, Y., Kogure, K., 1995. Rolipram, a cyclic AMP-selective phosphodiesterase inhibitor, reduces neuronal damage following cerebral ischemia in the gerbil. Eur. J. Pharmacol. 272, 107–110.

Kaufman, S., 1995. Tyrosine hydroxylase. Adv. Enzymol. Relat. Areas Mol. Biol. 70, 103–220.

Kaulen, P., Brüning, G., Schneider, H.H., Sarter, M., Baumgarten, H.G., 1989. Autoradiographic mapping of a selective cyclic adenosine monophosphate phosphodiesterase in rat brain with the anti-depressant [^{3}H]rolipram. Brain Res. 503, 229–245.

Lalli, E., Sassone-Corsi, P., 1994. Signal transduction and gene regulation: the nuclear response to cAMP. J. Biol. Chem. 269, 17359–17362.

McGeer, P.L., McGeer, E.G., 1995. The inflammatory response system of brain: implications for therapy of Alzheimer and other neurodegenerative diseases. Brain Res. Rev. 21, 195–218.

McGeer, P.L., McGeer, E., Rogers, J., Sibley, J., 1990. Anti-inflammatory drugs and Alzheimer's disease. Lancet 335, 1037.

Millhouse, O.E., 1987. Granule cells of the olfactory tubercle and the question of the Islands of Calleja. J. Comp. Neurol. 265, 1–24.

Millhouse, O.E., Heimer, L., 1984. Cell configurations in the olfactory tubercle of the rat. J. Comp. Neurol. 228, 571–597.

Morimoto, B.H., Koshland, D.E.J., 1991. Identification of cyclic AMP as the response regulator for neurosecretory potentiation: a memory model system. Proc. Natl. Acad. Sci. USA 88, 10835–10839.

Nieuwenhyus, R., Voogd, J., vanHuijzen, Chr, 1988. The Human Central Nervous System. Springer, Berlin, Heidelberg.

Obernolte, R., Ratzliff, J., Baecker, P.A., Daniels, D.V., Zuppan, P., Jarnagin, K., Shelton, E.R., 1997. Multiple splice variants of phosphodiesterase PDE4C cloned from human lung and testis. Biochem. Biophys. Acta 1353, 287–297.

Owens, R.J., Catterall, C., Batty, D., Jappy, J., Russell, A., Smith, B., O'Connell, J., Perry, M.J., 1997. Human phosphodiesterase 4A: characterization of full-length and truncated enzymes in COS cells. Biochem. J. 326, 53–60.

Parent, A., 1996. Carpenter's Human Neuroanatomy. Williams and Wilkins.

Paxinos, G., 1990. The Human Nervous System. Academic Press, Inc.

Paxinos, G., 1995. The Rat Nervous System, Second Edn. Academic Press.

Paxinos, G., Watson, C., 1998. The Rat Brain in Stereotaxic Coordinates, Fourth Edn. Academic Press.

Schneider, H.H., 1984. Brain cAMP response to phosphodiesterase inhibitors in rats killed by microwave irradiation or decapitation. Biochem. Pharmacol. 33, 1690–1693.

Schneider, H.H., Schmiechen, R., Brezinski, M., Seidler, J., 1986. Stereospecific binding of the antidepressant rolipram to brain protein structures. Eur. J. Pharmacol. 127, 105–115.

Silvestre, J.S., Fernández, A., Palacios, J.M., 1999a. Effects of rolipram on the elevated plus-maze test in rats: a preliminary study. J. Psychopharmacol. 13 (3), 274–277.

Silvestre, J.S., Fernández, A., Palacios, J.M., 1999b. Preliminary evidence,of an involvement of the cholinergic system in the sedative affects of rolipram in rats. Phamacol. Biochem. Behav. 64, 1–5.

Soderling, S.H., Beavo, J.A., 2000. Regulation of cAMP and cGMP signalling: new phosphodiesterases and new functions. Curr. Opin. Cell Biol. 12, 174–179.

Sommer, N., Löschmann, P.A., Northoff, G.H., Weller, M., Steinbrecher, A., Steinbach, J.P., Lichtenfels, R., Meyermann, R., Riethmüller, A., Fontana, A., Dichgans, J., Martin, R., 1995. The antidepressant rolipram suppresses cytokine production and prevents autoimmune encephalomyelitis. Nat. Med. 1, 244–248.

Stuart, A.M., Mitchell, I.J., Slater, P., Unwin, H.L.P., Crossman, A.R., 1986. A semi-quantitative atlas of 5-hydroxytryptamine-1 receptors in the primate. Brain Neurosci. 18, 619–639.

Szabo, J., Cowan, W.M., 1984. A stereotaxic atlas of the brain of the cynomolgus monkey (*Macaca fascicularis*). J. Comp. Neurol. 222, 265–300.

Takahashi, M., Terwilliger, R., Lane, C., Mezes, P.S., Conti, M., Duman, R.S., 1999. Chronic antidepressant administration increases the expression of cAMP-specific phosphodiesterase 4A and 4B isoforms. J. Neurosci. 19, 610–618.

Thompson, W.J., Appleman, M.M., 1971. Multiple cyclic nucleotide phosphodiesterase activities in rat brain. Biochemistry 10, 311–316.

Tomiyama, M., Palacios, J.M., Cortés, R., Vilaró, M.T., Mengod, G., 1997. Distribution of AMPA receptor subunit mRNAs in the human basal ganglia: an in situ hybridization study. Mol. Brain Res. 46, 281–289.

Torphy, T.J., Page, C., 2000. Phosphodiesterases: the journey towards therapeutics. Trends Pharmacol. Sci. 21, 157–159.

Watchel, H., 1983. Potential anti-depressant activity of rolipram and other selective cyclic adenosine 3′, 5′-monophosphate phosphodiesterase inhibitors. Neuropharmacology 22, 267–272.

Watchel, H., Schneider, H.H., 1986. Rolipram, a novel anti-depressant drug, reverses the hypothermia and hypokinesia of monoamine-depleted mice by an action beyond postsynaptic monoamine receptors. Neuropharmacology 25, 1119–1126.

Yamashita, N., Hayashi, A., Baba, J., Aawa, A., 1997. Rolipram, a phosphodiesterase-4-selective inhibitor, promotes the survival of cultured rat dopaminergic neurons. Jpn. J. Pharmacol. 75, 155–159.

Zeller, E., Stief, H.J., Plug, B., Sastre-y-Hemandez, M., 1984. Results of a phase II study of the anti-depressant effect of rolipram. Pharmacopsychiatry 17, 188–190.

Zhong, Y., Wu, C.F., 1991. Altered synaptic plasticity in drosophila memory mutants with a defective cyclic AMP cascade. Science 251, 198–201.